

## Igneous Rock Associations 4. Oceanic Island Volcanism I Mineralogy and Petrology

John D. Greenough, Jaroslav Dostal and Leanne M. Mallory-Greenough

Volume 32, Number 1, March 2005

URI: [https://id.erudit.org/iderudit/geocan32\\_1ser01](https://id.erudit.org/iderudit/geocan32_1ser01)

[See table of contents](#)

Publisher(s)

The Geological Association of Canada

ISSN

0315-0941 (print)

1911-4850 (digital)

[Explore this journal](#)

Cite this article

Greenough, J. D., Dostal, J. & Mallory-Greenough, L. M. (2005). Igneous Rock Associations 4. Oceanic Island Volcanism I Mineralogy and Petrology. *Geoscience Canada*, 32(1), 29–45.

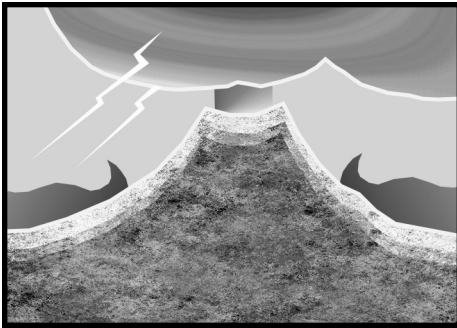
Article abstract

Oceanic islands tend to occur at the young ends of hotspot trails because they record the passage of oceanic plates over rising convection cells (plumes) in the mantle, or the propagation of cracks in the lithosphere. Basaltic volcanism on oceanic islands is generally unexplosive and, although potentially destructive, poses less threat to human life than volcanism in other tectonic environments. However, the possibility of giant tsunamis from the catastrophic gravitational collapse of islands is of real concern for major cities surrounding the ocean basins.

Two series of magmas are recognized in oceanic islands. Tholeiites form at lower pressures than alkali basalts, from higher percentages of decompression melting. The former contain a low-Ca pyroxene and the latter can crystallize nepheline. Furthermore, minerals common to both series (chromite, olivine, augite, plagioclase, magnetite and ilmenite) are compositionally distinct reflecting fundamental chemical differences between the two magma series.

Mineral compositions vary as magmas evolve in sub-volcanic, lithospheric magma chambers by assimilation and differentiation. Magmas assimilate wall rocks in these chambers. Time-scales for differentiation (mostly crystal fractionation) are generally less than a few thousand years. Early olivine, pyroxene, chromite and immiscible sulfide formation cause compatible elements (e.g., Ni, Co, Cr) to decline rapidly as differentiation proceeds. Plagioclase dramatically removes Sr at intermediate stages and alkali feldspars sequester Ba and Rb as late-stage trachytes and phonolites form in alkaline magmas. The high-field-strength elements are generally incompatible but locally decline reflecting apatite (P) and Fe-Ti oxide (Ti, Nb, Ta) removal. Studies of layering in individual lava flows suggest that rising volatiles may effect mass transfer of complexed ions during differentiation in magma chambers.

# SERIES



## Igneous Rock Associations 4. Oceanic Island Volcanism I Mineralogy and Petrology

John D. Greenough<sup>1</sup>, Jaroslav Dostal<sup>2</sup>, and Leanne M. Mallory-Greenough<sup>3</sup>

<sup>1</sup>Department of Earth and Environmental Sciences, University of British Columbia - Okanagan, 3333 University Way, Kelowna, BC, V1V 1V7. E-mail: jdgreeno@ouc.bc.ca  
Tel: 250 762 5445 ext. 7520; Fax: 250 470 6005

<sup>2</sup>Department of Geology, Saint Mary's University, Halifax, NS, B3H 3C3. E-mail: jdostal@smu.ca

<sup>3</sup>Department of Geology, University of Toronto, 22 Russell St., Toronto, ON, M5S 3B1. E-mail: mallory@ouc.bc.ca

### SUMMARY

Oceanic islands tend to occur at the young ends of hotspot trails because they record the passage of oceanic plates over rising convection cells (plumes) in the mantle, or the propagation of cracks in the lithosphere. Basaltic volcanism on oceanic islands is generally unexplosive and, although potentially destructive, poses less threat to human life than volcanism in other tectonic

environments. However, the possibility of giant tsunamis from the catastrophic gravitational collapse of islands is of real concern for major cities surrounding the ocean basins.

Two series of magmas are recognized in oceanic islands. Tholeiites form at lower pressures than alkali basalts, from higher percentages of decompression melting. The former contain a low-Ca pyroxene and the latter can crystallize nepheline. Furthermore, minerals common to both series (chromite, olivine, augite, plagioclase, magnetite and ilmenite) are compositionally distinct reflecting fundamental chemical differences between the two magma series.

Mineral compositions vary as magmas evolve in sub-volcanic, lithospheric magma chambers by assimilation and differentiation. Magmas assimilate wall rocks in these chambers. Time-scales for differentiation (mostly crystal fractionation) are generally less than a few thousand years. Early olivine, pyroxene, chromite and immiscible sulfide formation cause compatible elements (e.g., Ni, Co, Cr) to decline rapidly as differentiation proceeds. Plagioclase dramatically removes Sr at intermediate stages and alkali feldspars sequester Ba and Rb as late-stage trachytes and phonolites form in alkaline magmas. The high-field-strength elements are generally incompatible but locally decline reflecting apatite (P) and Fe-Ti oxide (Ti, Nb, Ta) removal. Studies of layering in individual lava flows suggest that rising volatiles may effect mass transfer of complexed ions during differentiation in magma chambers.

### SOMMAIRE

Les îles océaniques se trouvent généralement à l'extrémité la plus jeune des traînées de points chauds parce qu'elles sont la marque du passage de plaques

océaniques au-dessus de cellules de convection ascendantes (panaches) dans le manteau ou de la propagation de fissures de la lithosphère. En général, le volcanisme basaltique des îles océaniques n'est pas explosif, et bien qu'il puisse être destructeur, il présente moins de danger pour les humains que le volcanisme d'autres environnements tectoniques. Cependant, la formation possible de tsunamis géants provoqués par l'effondrement d'îles constitue un danger réel pour les grandes agglomérations situées au pourtour des bassins océaniques.

On distingue deux séries magmatiques dans les matériaux constitutifs des îles océaniques. Les tholéiites qui se forment à des pressions plus faibles que les basaltes alcalins, et plus souvent sous des conditions de fusion par décompression, et les basaltes alcalins. Les premières contiennent un pyroxène à faible teneur en calcium et l'autre permet la cristallisation de la néphéline. De plus, les minéraux communs à ces deux séries (chromite, olivine, augite, plagioclase, magnétite et ilménite) ont des compositions distinctes qui reflètent les différences de composition chimique intrinsèques de ces deux séries magmatiques.

Les compositions minérales varient puisque les magmas changent de composition dans les chambres magmatiques lithosphériques pré-volcaniques par assimilation et différenciation. Les magmas absorbent les roches des murs d'enceinte dans ces chambres. Les échelles de temps de ces différenciations (principalement de fractionnement cristallin) s'étalent généralement sur quelques milliers d'années. D'abord, la formation d'olivine, de pyroxène, de chromite et de sulfures immiscibles entraîne un appauvrissement rapide du magma en éléments compatibles (Ni, Co, Cr par ex.). Puis, aux stades inter-

médiaires, la formation de plagioclases réduit considérablement la teneur en Sr et, aux stades finaux, la formation de feldspaths alcalins en extrait le Ba et le Rb alors que se forment les trachytes et les phonolites à partir de magmas alcalins. Les éléments les plus fortement polarisés sont généralement incompatibles mais, localement, leur teneur décline, reflétant ainsi la formation d'apatite (P) et d'oxydes de Fe-Ti (Ti, Nb, Ta). Les résultats d'études sur la formation en couche de coulées de laves indiquent que l'ascension gravitationnelle des volatils pourrait avoir un effet sur le transfert de masse d'ions complexes durant la différenciation dans les chambres magmatiques.

## INTRODUCTION

Most igneous activity in the ocean basins occurs at plate boundaries. Ocean-floor basalts are extruded along mid-ocean ridges that define divergent boundaries, whereas island-arcs are produced as the ocean floor is subducted at convergent plate boundaries. In contrast, oceanic island, oceanic plateau and seamount volcanism is distinctive in composition

and eruptive style from the activity at plate margins. These sub-sea and subaerial land forms represent <1 % of all igneous rocks on Earth and ~2% of all volcanic activity in the deep ocean basins. However, enormous emphasis has been placed on them for understanding igneous processes and the evolution of Earth. Separated from contaminating continental crust, and unaltered by mountain-building metamorphic and tectonic processes (Basaltic Volcanism Study Project = BVSP, 1981, p. 161), oceanic island basalts (OIB) provide insights into mantle composition, magma formation processes and magma evolution (Fig. 1).

The significance of oceanic islands is apparent in any literature review. Their archipelagoes led to the formulation of fundamental plate tectonic ideas (Wilson, 1963), have influenced hypotheses for how convection drives plate tectonics (Morgan, 1971; Wilson, 1973; Hamilton, 2003), and today fuel a healthy debate about chemical layering in the Earth (Anderson, 1999; Allègre, 2002). Further, the gravitational instability of oceanic islands

indicates that collapses could imperil major cities bordering the ocean basins (McGuire, 1996). Thus, studies of oceanic islands have both intellectual and hazard-alleviation significance for humans.

This is the first of two complementary papers on oceanic island basalts. It reviews the mineralogy, classification, tectonic significance and lithospheric processes (e.g., differentiation) affecting OIB magmas. The second paper (Greenough et al., in press) examines the mantle processes affecting OIB magma generation, including the influence of source mineralogy and the effects of fluids and percentage melting on magma composition; it also provides isotopic and trace element evidence for five distinct types of mantle source regions. All aspects of oceanic island rocks, including petrography, volcanology, and geochemistry, are inter-related. Thus, no one scale of observation is entirely satisfactory to understanding their origin. This paper begins with hand-specimen scale features, and ends with the effect of differentiation processes on magmas.

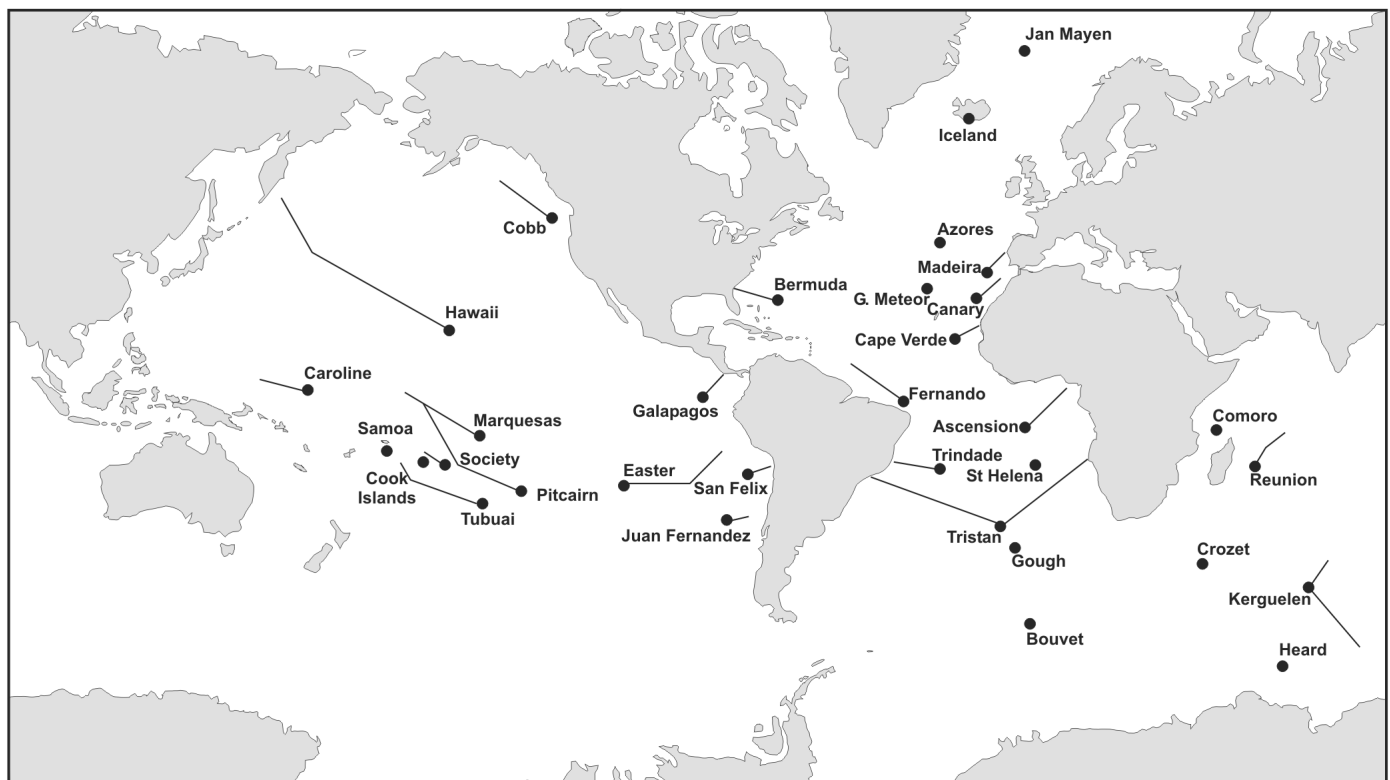


**Figure 1.** Map showing oceanic islands and island chains in the ocean basins (modified from Crough, 1983). Chains (shown) with islands discussed in text include: Azores chain (Sao Miquel and Faial islands); Canary Islands (Gran Canaria and Tenerife); Galapagos (Floreana and Isabela); Samoa (Tutuila and Upolu); Hawaii (Kauai, Hawaii and Loihi); Society Islands (Tahiti); Marquesas Islands (Eiao); Cook Islands (Aitutaki and Mangaia); and Comores (Grande Comore).

**PETROGRAPHY AND MINERALOGY**

Oceanic island rocks form two major families based on mineralogy and petrography: those that form from tholeiitic basalts and those from alkali basalts. Mantle-melting processes lead to chemical gradation between the two, but under low-pressure conditions in the lithosphere, each basalt type crystallizes different minerals and evolves in very different ways.

Alkali basalts and tholeiites are theoretically distinguished from each other using their modal mineralogy (Fig. 2; Table 1). However, many volcanic rocks are completely glass, or are extremely fine grained, making mineral identification impossible or difficult. To overcome this problem, a whole-rock major-element analysis is used to calculate the normative mineralogy, which estimates the abundances of minerals that would have formed if the rock crystallized (cf. Philpotts, 1990, pp. 88-92). All basalt chemical compositions can be plotted in the basalt tetrahedron, which has normative quartz, olivine, nepheline and augite at the apices. Because all basalts contain augite (modal or normative), compositions are projected onto the Ne-Q-Ol plane (Fig. 3). Alkali basalts are separated from tholeiitic basalts by the Ol-Ab join. This line has great significance, because, if Figure 3 was converted into a phase diagram, the Ol-Ab join would approximately coincide with a high-temperature line or “thermal divide”. As any basalt cools and crystallizes minerals under low-pressure conditions, the left-over (residual) liquid’s composition moves down-temperature, away from the thermal divide and Ol-Ab join. Thus, once in the lithosphere (low pressure), the composition of magmas cannot generally cross this line resulting in two series of magmas, tholeiites (Hy side of Ol-Ab join) and alkali basalts (Ne side).

The most fundamental characteristic of tholeiites is the presence of a low-Ca pyroxene (e.g., hypersthene), most commonly in the matrix, locally as phenocrysts (Fig. 2a), or as calculated in the norm. Thus, tholeiites fall in the Ol-Ab-Hy or Q-Ab-Hy triangles of the basalt tetrahedron (Fig. 3). Unfortunately, rocks plotting close the Ol-Ab join can have small percentages of normative Hy but no modal low-Ca pyroxene. The thermal divide and Ol-Ab

normative mineralogy join do not precisely coincide. Various factors, including magma composition, control whether orthopyroxene or pigeonite occurs as the low-Ca pyroxene, but high temperatures yield orthopyroxene and low-pressure crystallization favours pigeonite. Only tholeiites can have quartz, which, if present, is usually restricted to the matrix. The most common phenocryst silicate phases are olivine, plagioclase and augite, typically, although not always, appearing in that order (Fig. 2b).

Alkali basalts (Table 1) contain nepheline (Fig. 2d), commonly only in the norm, and plot in the Ol-Ne-Ab triangle of the tetrahedron (Fig. 3). Basanites contain modal nepheline. Less commonly, mantle melting yields magma with such low silica activity that plagioclase cannot form. These rocks, nephelinites, only contain nepheline ± melilite. Ultramafic xenoliths primarily occur only in alkali basalts. The most common phenocryst phases are the same as those in tholeiites, but tend to form in the order olivine, augite and plagioclase. Augite is generally complexly

zoned and pleochroic and has Ti-rich rims (Fig. 2c). Both alkali and tholeiitic basalts contain chromite as an early crystallizing phase, and form magnetite and/or ilmenite over a large range of temperatures.

**MINERAL CHEMISTRY**

Mineral compositions are closely connected to magma alkalinity (degree of silica saturation or undersaturation), the sequence of mineral crystallization and degree of magma evolution. Table 2 contains representative analyses of major silicate phases discussed below (see supplementary materials at <http://www.gac.ca/JOURNALS/geo-can.html> for references and islands represented on plots).

**Spinel**

Spinel (chromite) is an early crystallizing phase in oceanic island basalts (OIB). Alkali basalt chromites tend to show higher Cr<sub>2</sub>O<sub>3</sub>, Al<sub>2</sub>O<sub>3</sub>, and MgO, but lower TiO<sub>2</sub> than tholeiites at comparable Cr<sub>2</sub>O<sub>3</sub>/Al<sub>2</sub>O<sub>3</sub> ratios (Fig. 4). The trends shown in Figures 4a and 4b reflect dif-

**Table 1:** Petrographic and mineralogical characteristics of alkali and tholeiitic basalts.

| Alkali Basalts   | Tholeiitic Basalts   |
|--|--|
| Contain normative or modal nepheline   | Nepheline absent.  |
| Biotite may be present in the matrix.  | Biotite absent.  |
| Interstitial alkali feldspar present but difficult to identify.  | No modal alkali feldspar.  |
| In rare cases there is modal analcite.   | No modal analcite.   |
| Low-Ca-pyroxene (pigeonite or orthopyroxene) absent.   | Contain a low-Ca-pyroxene (pigeonite or orthopyroxene) in the norm or mode.  |
| Quartz absent.   | Quartz may be present in the matrix.   |
| Olivine occurs in most samples, phenocrysts zoned with Fe-rich rims.   | Olivine phenocrysts less common, generally unzoned, and may have a low-Ca-pyroxene reaction rim. Olivine missing from matrix.            |
| Augite phenocrysts more strongly pleochroic having purplish-brown, Ti-rich rims.   | Augite phenocrysts generally pale-brown and zoning is not as apparent as in alkali basalts.  |
| Phenocryst sequence = olivine, augite, plagioclase such that plagioclase phenocrysts are less common than in tholeiites. | Phenocryst sequence = olivine, plagioclase, augite locally yielding ophitic and subophitic textures typical of most terrestrial basalts. |
| Coarser grained with mafic pegmatites common in segregation veins even in thin flows.                                    | Finer grained, intergranular textures compared to alkaline flows of comparable thickness.  |
| Ultramafic xenoliths common.   | Ultramafic xenoliths extremely rare.   |

Notes: Modified from Hughes, 1982, p. 297.

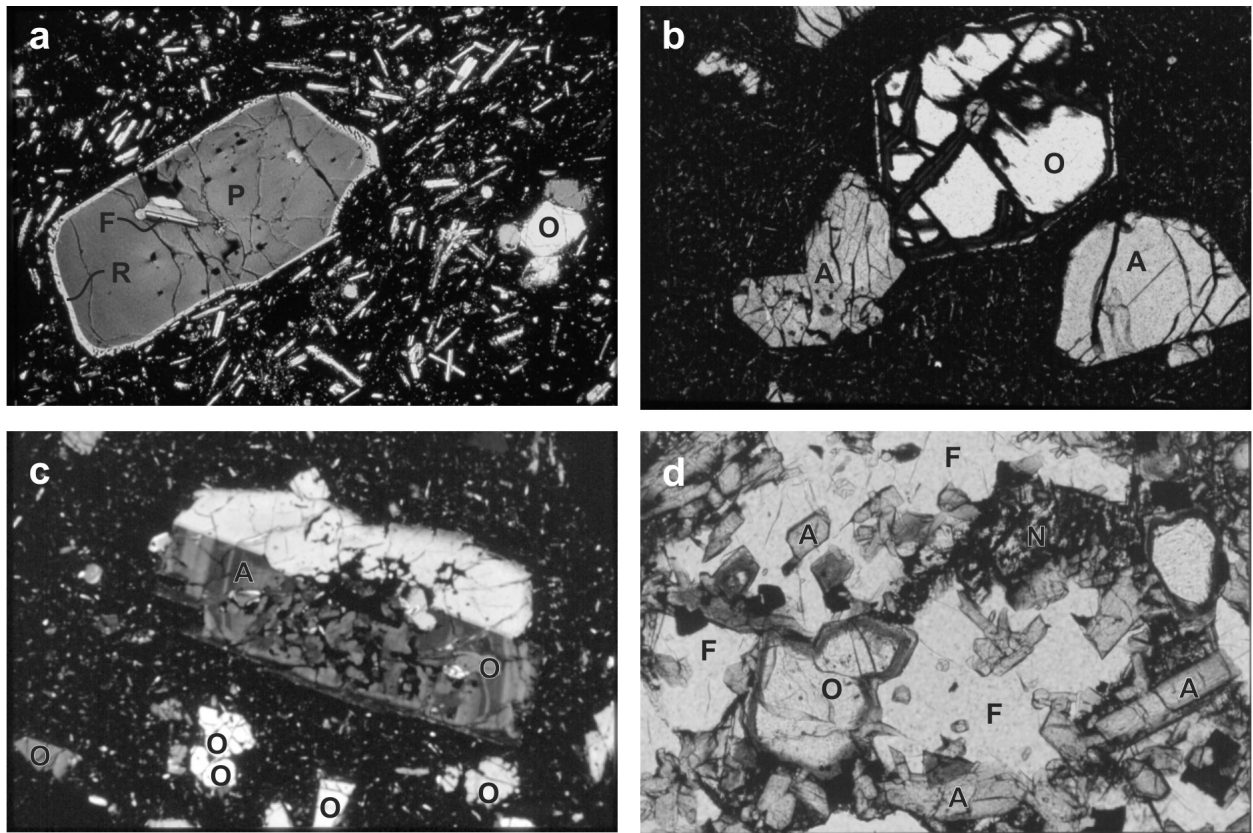


**Figure 2.** Photomicrographs of oceanic-island-tholeiites (a, b) and alkali basalts (c, d). a) Mauna Loa (Hawaii) tholeiite with a large (3.2 mm long) orthopyroxene phenocryst ( $\text{En}_{70}$ ; P on photo) and group of 4 smaller ( $<0.7$  mm) unzoned olivine phenocrysts ( $\sim\text{Fo}_{70}$ ; O). The orthopyroxene contains plagioclase inclusions (F) and is unzoned except for a thin Fe-rich rim (R) (crossed polars; 5.1 mm wide). b) Upolu (Samoa) tholeiite with a euhedral, diamond-shaped, unzoned ( $\text{Fo}_{67}$ ) olivine phenocryst (1.3 mm wide; marked O) and slightly pleochroic (darker coloured) augite phenocrysts (A) in a very fine-grained matrix typical of tholeiites. The lack of plagioclase phenocrysts suggests plagioclase was a late-forming phase. Olivine shows iddingsite alteration on the rim and along fractures (plane-polarized light; photo = 2.6 mm wide). c) Tenerife (Canaries) alkali basalt with large (4.6 mm), twinned, complexly zoned (variable concentric shading), and included (olivine = O) augite phenocryst (A) surrounded by a fine-grained matrix having smaller phenocrysts of olivine (= O;  $\text{Fo}_{80}$ ). The zoning and Ti-rich rim (barely visible, thin, dark edge) on augite are typical alkali-basalt features (crossed polars; photo = 2.6 mm wide). d) Kauai (Hawaii) alkali basalt with euhedral olivine (O; 0.25 mm;  $\text{Fo}_{80}$ ) and augite phenocrysts (A,  $\leq 0.3$  mm long) the latter locally surrounded by irregular plagioclase (F) masses. Dark, polygonal-shaped areas of mesostasis contain serrated Fe-Ti oxides and apatite needles intergrown with nepheline (N) typical of alkali basalts. The olivine phenocryst has an iddingsite alteration rim. Some augite grains show a thin, darker coloured rim reflecting high Ti content (plane-polarized light; photo = 1.3 mm wide). Mineral compositions determined optically.

ferentiation; as the  $\text{Cr}_2\text{O}_3/\text{Al}_2\text{O}_3$  ratios drop,  $\text{Cr}_2\text{O}_3$  decreases,  $\text{Al}_2\text{O}_3$  rises (BVSP, 1981, p. 179) and  $\text{TiO}_2$  apparently decreases in the alkali basalts, but increases in the tholeiites.

### Olivine

Olivine precipitation appears to begin and end early in tholeiite rock suites creating a restricted range of olivine Fo contents (e.g.,  $\text{Fo}_{90}$  -  $\text{Fo}_{70}$  for Kilauean tholeiites). Precipitation over a greater temperature range in the alkali basalts yields more variation in the Fo contents (BVSP, 1981, p. 179). Nevertheless, some tholeiites can show a large range

of olivine compositions ( $\sim\text{Fo}_{90}$  -  $\text{Fo}_{40}$ ; Fig. 5). Zoned crystals, which are more common in alkali basalts, generally have Fe-rich rims. Minor components in olivine include CaO, MnO,  $\text{Al}_2\text{O}_3$ ,  $\text{Cr}_2\text{O}_3$  and NiO. The highest Ca contents mostly occur in alkali-basalt olivines (Fig. 5). Nickel is strongly concentrated in olivine relative to the coexisting magma ( $K_D \sim 19$ , depending on magma MgO) and the variations in magma Ni concentrations act as sensitive indicators of olivine precipitation.

### Augite

Le Bas (1962) showed that lower mag-

matic Si contents in alkali basalts, when compared to tholeiites, can cause more Al to substitute for Si in augite tetrahedral sites. To maintain charge balance, high-valency cations, such as  $\text{Al}^{3+}$  and  $\text{Ti}^{4+}$  enter octahedral sites normally occupied by divalent cations (e.g.,  $\text{Mg}^{2+}$  and  $\text{Fe}^{2+}$ ). Thus,  $\text{Al}_2\text{O}_3$  (Fig. 6a) and  $\text{TiO}_2$  tend to be higher in alkali-basalt augites. The minor components MnO and  $\text{Na}_2\text{O}$  help distinguish magma types (Nisbet and Pearce, 1977) with the former lower and the latter higher in alkali-basalt augites (Fig. 6b). Higher  $\text{Na}_2\text{O}$  in alkali-basalt augites may reflect higher magmatic alkali contents or a charge-bal-

Table 2: Example analyses of major silicate minerals in alkali and tholeiitic basalts.

| Mineral                        | Olivine   | Olivine  | Augite    | Augite   | Opx       | Opx       | Plag      | Plag     | Nepheline |
|--------------------------------|-----------|----------|-----------|----------|-----------|-----------|-----------|----------|-----------|
| Series                         | Tholeiite | Alkaline | Tholeiite | Alkaline | Tholeiite | Tholeiite | Tholeiite | Alkaline | Alkaline  |
| Island                         | Iceland   | Gr.Com.  | Iceland   | Gr.Com.  | Haw ML    | Haw K     | Haw ML    | Gr. Com  | Tubuai    |
| Sample                         | TH-4      | MA-1     | GR-22     | 13       | 184-1     | KP26S1    | 183-14    | MA-17    | TU 4      |
| SiO <sub>2</sub>               | 39.11     | 37.54    | 51.81     | 50.84    | 54.92     | 53.8      | 49.9      | 58.03    | 44.11     |
| TiO <sub>2</sub>               |           |          | 0.85      | 0.88     | 0.34      | 0.66      |           |          |           |
| Al <sub>2</sub> O <sub>3</sub> |           |          | 2.02      | 3.99     | 1.92      | 1.02      | 31.4      | 26.44    | 33.75     |
| Cr <sub>2</sub> O <sub>3</sub> |           |          | 0.15      | 0.44     |           | 0.05      |           |          |           |
| FeO                            | 15.97     | 24.33    | 8.78      | 5.02     | 10.79     | 16.7      | 0.70      | 0.32     | 0.91      |
| CaO                            | 0.33      | 0.20     | 19.71     | 21.63    | 2.32      | 2.37      | 15.1      | 8.98     | 0.04      |
| MgO                            | 43.93     | 36.99    | 14.85     | 15.7     | 29.1      | 25.4      |           | 0.06     |           |
| MnO                            | 0.23      | 0.33     | 0.16      | 0.10     | 0.22      | 0.30      |           |          |           |
| NiO                            |           | 0.17     |           |          |           |           |           |          |           |
| K <sub>2</sub> O               |           |          |           | 0.02     |           |           | 0.07      | 0.49     | 4.82      |
| Na <sub>2</sub> O              |           |          | 0.30      | 0.34     | 0.03      | 0.05      | 2.63      | 5.89     | 16.88     |
| Sum                            | 99.57     | 99.56    | 98.63     | 98.96    | 99.64     | 100.35    | 99.8      | 100.21   | 100.51    |
| Si                             | 0.993     | 0.993    | 1.947     | 1.886    | 1.952     | 1.955     | 9.142     | 10.386   | 8.396     |
| Ti                             |           |          | 0.024     | 0.025    | 0.009     | 0.018     |           |          |           |
| Al                             |           |          | 0.089     | 0.174    | 0.080     | 0.044     | 6.780     | 5.577    | 7.571     |
| Cr                             |           |          | 0.004     | 0.013    |           | 0.001     |           |          |           |
| Fe                             | 0.339     | 0.538    | 0.276     | 0.156    | 0.321     | 0.507     | 0.107     | 0.048    | 0.145     |
| Ca                             | 0.009     | 0.006    | 0.793     | 0.859    | 0.088     | 0.092     | 2.964     | 1.722    | 0.008     |
| Mg                             | 1.662     | 1.459    | 0.832     | 0.868    | 1.542     | 1.376     |           | 0.016    |           |
| Mn                             | 0.005     | 0.007    | 0.005     | 0.003    | 0.007     | 0.009     |           |          |           |
| Ni                             |           | 0.004    |           |          |           |           |           |          |           |
| K                              |           |          |           | 0.001    |           |           | 0.016     | 0.112    | 1.170     |
| Na                             |           |          | 0.022     | 0.024    | 0.002     | 0.004     | 0.934     | 2.044    | 6.229     |
| Total                          | 3.007     | 3.007    | 3.993     | 4.009    | 4.000     | 4.006     | 19.943    | 19.904   | 23.518    |
| Fo%                            | 83.1      | 73.1     |           |          |           |           |           |          |           |
| Ca%                            |           |          | 41.7      | 45.6     | 4.5       | 4.7       |           |          |           |
| Mg%                            |           |          | 43.8      | 46.1     | 79.0      | 69.6      |           |          |           |
| Fe%                            |           |          | 14.5      | 8.3      | 16.4      | 25.7      |           |          |           |
| Ca%                            |           |          |           |          |           |           | 75.7      | 44.4     |           |
| K%                             |           |          |           |          |           |           | 0.4       | 2.9      |           |
| Na%                            |           |          |           |          |           |           | 23.9      | 52.7     |           |

**Notes:** Major-element oxides in wt.% with total Fe as FeO. Formulas for olivine, augite, orthopyroxene (Opx), plagioclase (Plag) and nepheline calculated on the basis of 4, 6, 6, 32 and 32 oxygen, respectively.

Mole proportions of endmember components are given at the bottom of each column (except for nepheline).

Island abbreviations: Gr. Com = Grande Comore; Haw ML = Hawaii, Mauna Loa; Haw K = Hawaii, Kilauea.

Reference citations appear in supplementary materials online at <http://www.gac.ca/JOURNALS/geocan.html>: Sample TH 4 & GR-22 = Mäköpää, 1978; MA-1 & MA-17 = Spaeth et al., 1996; 13 = Strong, 1972; 184-1 & 183-14 = Garcia et al. 1995; KP-26 Scoria 1 = Wright and Helz, 1996; TU 4 = Brousse and Maury, 1980.

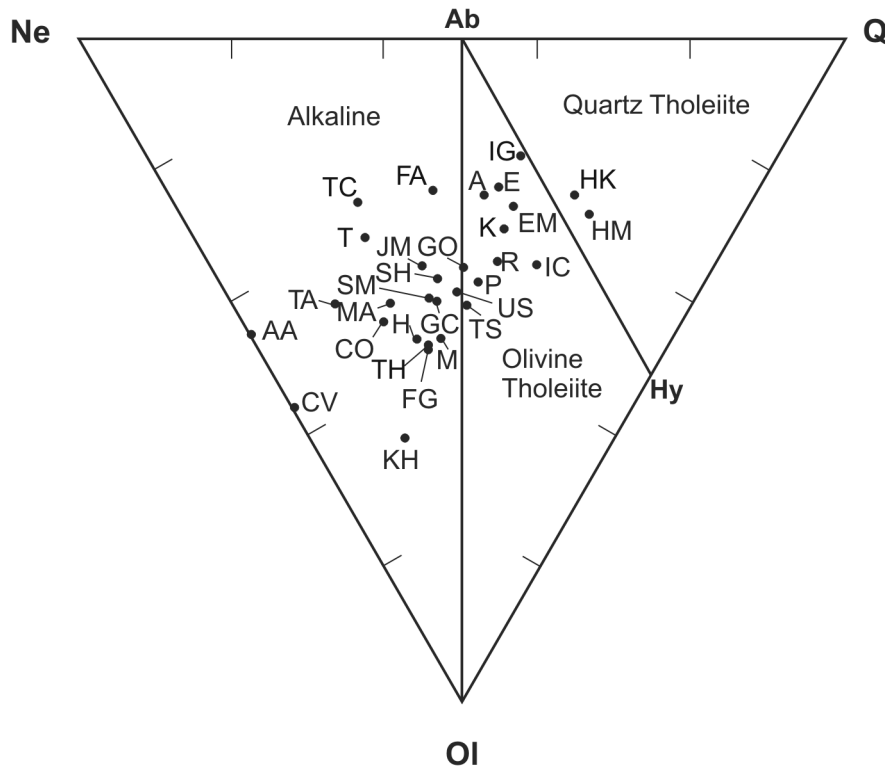


**Figure 3.** The normative composition of oceanic-island-basalts projected from diopside onto the base of the basalt tetrahedron. OI = normative olivine, Ne = nepheline, Q = quartz, Ab = albite, and Hy = normative hypersthene. Molecular norms ( $\text{Fe}^{3+}/\text{Fe}^{2+}$  adjusted to 0.30 atomic) calculated from averaged data for basalts with  $\text{Mg}\# \geq 0.40$  and  $\leq 0.77$ . Island symbols: A = Ascension; AA = Aitutaki, Austral-Cook Islands; CO = Grande Comore, Comoros; CV = Cape Verde; E = Easter Island; EM = Eiao, Marquesas; FA = Faial, Azores; FG = Floreana, Galapagos; GC = Gran Canaria, Canaries; GO = Gough; H = Heard Island; HK = Kilauea Volcano, Hawaii; HM = Mauna Loa Volcano, Hawaii; IC = Iceland; IG = Isabela, Galapagos; JM = Jan Mayen; K = Kergulen; KH = Kauai, Hawaii; M = Madeira; MA = Mangaia, Austral-Cook Islands; P = Pitcairn; R = Reunion; SH = St. Helena; SM = Sao Miquel, Azores; T = Tristan da Cunha; TA = Tubuai, Austral-Cook Islands; TC = Tenerife, Canaries; TH = Tahiti, Societies; TS = Tutuila, Samoa; US = Upolu, Samoa. Data and references in supplementary materials online at <http://www.gac.ca/JOURNALS/geocan.html>.

ance response to high-charge-density  $\text{Al}^{3+}$  and  $\text{Ti}^{4+}$  cations entering octahedral sites. Low-oxygen fugacities cause Fe to be enriched in residual magma as tholeiites differentiate, because Fe-oxide formation is inhibited. A similar enrichment in magmatic MnO may cause high MnO in tholeiitic augites. The Ca contents of tholeiitic augites are lower reflecting the dilution of the diopside-hedenbergite molecule by a low-Ca pyroxene molecule (Fig. 7). There are also differences in how augite compositions change as differentiation proceeds. In alkali basalts, they move parallel to the diopside-hedenbergite join. In tholeiites, the Ca proportion drops until the Mg:Fe ratio reaches  $\sim 1:1$ , at which point

Ca begins rising again as the hedenbergite component goes up.

### Low-Ca Pyroxenes

In addition to augite, tholeiites also contain low-Ca pyroxenes (Fig. 7). Orthopyroxene forms in primitive (high-MgO) basalts but as differentiation proceeds, it is replaced by pigeonite once the enstatite component falls below 60 to 70 atomic percent. There is a miscibility gap between augite and the low-Ca pyroxenes making compositions that plot between the two less common (Fig. 7). However, rapid crystallization (quenching) can yield disequilibrium compositions (sub-calcic augites) which plot in the miscibility

gap is narrower at high temperatures, so that under slow cooling conditions, early formed augites and low-Ca pyroxenes develop exsolution lamellae as low-Ca pyroxene and augite (respectively) are expelled from the structures. Coexisting low- and high-Ca pyroxene compositions are related to temperature allowing two-pyroxene geothermometry (Davidson and Lindsley, 1985). For example, in Fig. 7 the long-dashed line between the Skaergaard trend lines connects coexisting pyroxenes formed at  $\sim 1000^\circ\text{C}$ .

### Plagioclase

Higher alkali-metal concentrations in alkali basalts result in plagioclases having higher  $\text{K}_2\text{O}$  values (represented by higher molecular orthoclase; Fig. 8) than those in tholeiites. Except for K and Fe, few elements substitute for the major cations (Ca, Na, Al, Si) in high-enough concentrations for routine analysis (e.g., by electron microprobe). As temperatures drop and differentiation proceeds, Na substitutes for Ca with coupled substitution of Si for Al to maintain charge balance. Thus most compositional variation reflects differentiation. Compared to augite, plagioclase is rarely used as an indicator of magma type, perhaps because there are few measurable minor components. However, multiple analyses yield information that not only reflects magma type, but can “fingerprint” individual lava flows (Mallory-Greenough et al., 2002).

### Magnetite and Ilmenite

Like Cr-rich spinels, magnetites from tholeiitic basalts tend to show lower  $\text{Al}_2\text{O}_3$  and  $\text{Cr}_2\text{O}_3$  and higher  $\text{TiO}_2$  concentrations than those with comparable  $\text{Cr}_2\text{O}_3/\text{Al}_2\text{O}_3$  in alkali basalts (Figs. 4a, c, d). However, ilmenites from tholeiites tend to have lower  $\text{Al}_2\text{O}_3$  and lower  $\text{TiO}_2$  concentrations (Fig. 9). The compositions of coexisting magnetite and ilmenite can be used to estimate liquidus temperatures and oxygen fugacity (Andersen and Lindsley, 1988) of magmas, although subsolidus exsolution produces intergrowths that complicate application of the geothermometer/oxygen barometer in slowly cooled, coarse-grained rocks.

**TECTONIC SETTING AND MANTLE CONVECTION**

Oceanic-island volcanism occurs at the ends of hotspot trails (e.g., Hawaiian-Emperor), which can, in places, be traced, using seamounts, across major parts of ocean basins (Fig. 1). The volcanically active trail-ends are preferentially located near divergent plate boundaries and are rare near convergent boundaries (Zhao, 2001). Wilson (1963) proposed that the trails reflect movement of oceanic plates over fixed mantle

hotspots, an idea central to acceptance of plate tectonic theory. Many scientists think that hotspots mark locations where diapiric convection cells, called mantle “plumes”, rise beneath lithospheric plates (Morgan, 1971; Wilson, 1973). Detailed studies of the angular relationships of hotspot trails show that the distance to the north magnetic pole, and by assumption the north geographic pole (= spin axis), has changed by up to 8 mm/y over the past 100 Ma, providing evidence for “true polar wander” or

movement of hotspots relative to the geographic pole (Duncan and Richards, 1991). Also, hotspots probably move relative to one another and this is consistent with fixed hotspots being unlikely, if “plume” models for convection in the mantle are correct (Koppers et al., 2001). Nevertheless, these conclusions do not negate the hypothesis that hotspot trails dominantly reflect plate motions. Despite the popularity of the plume model, hotspots (oceanic islands) may simply represent the position of propa-

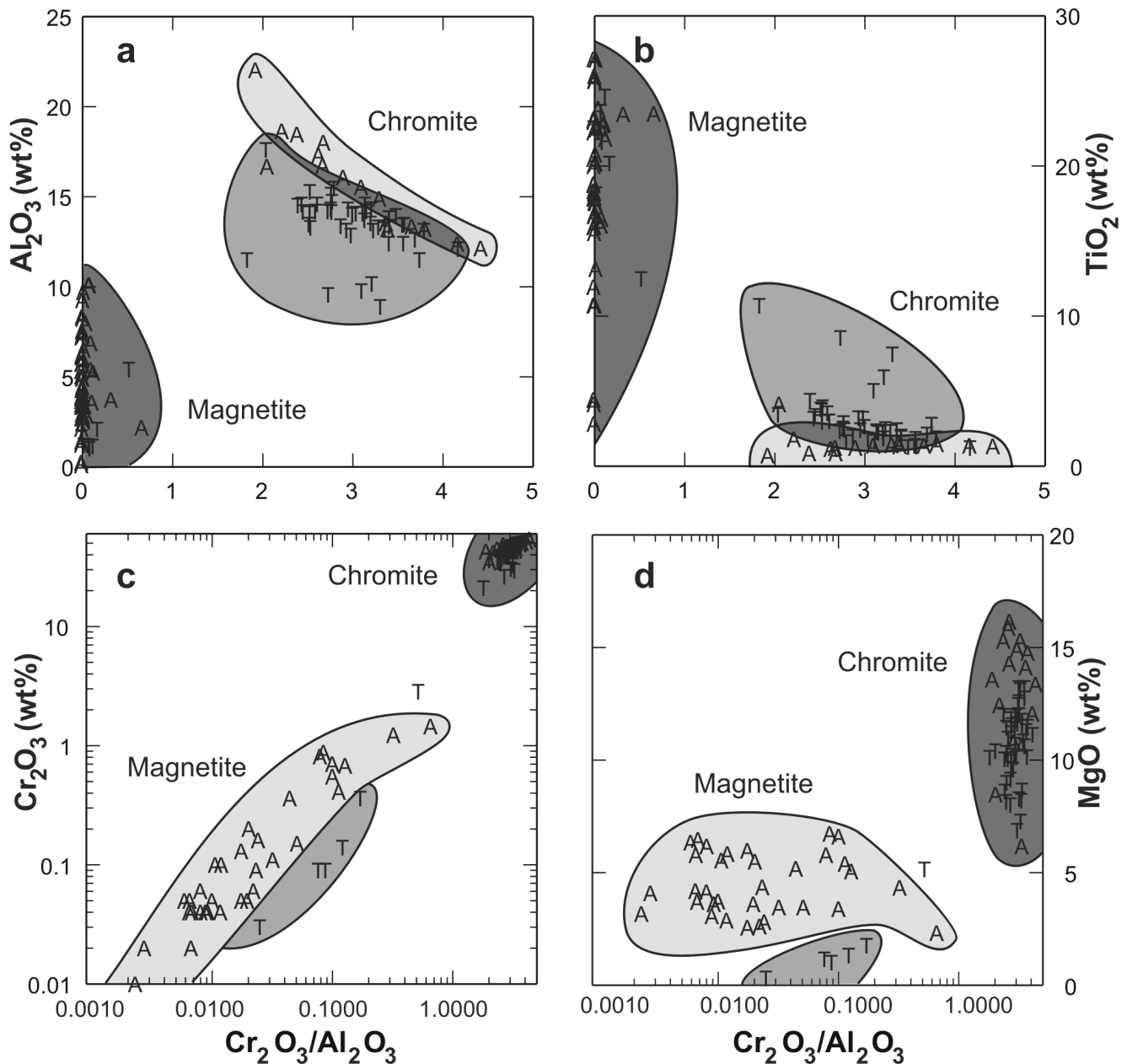


**Figure 4.** Plots of  $Cr_2O_3/Al_2O_3$  (oxide wt. % / oxide wt. %) versus the concentrations (oxide wt. %) of  $Al_2O_3$ ,  $TiO_2$ ,  $Cr_2O_3$  and  $MgO$  (diagrams a, b, c and d respectively) in chromites ( $Cr_2O_3/Al_2O_3 > 1$ ) and magnetites from alkali (A symbols) and tholeiitic (T) basalts. Note the log scale for  $Cr_2O_3$  concentrations in diagram c and for  $Cr_2O_3/Al_2O_3$  in diagrams c and d. Data references and islands in supplementary materials online at <http://www.gac.ca/JOURNALS/geocan.html>.



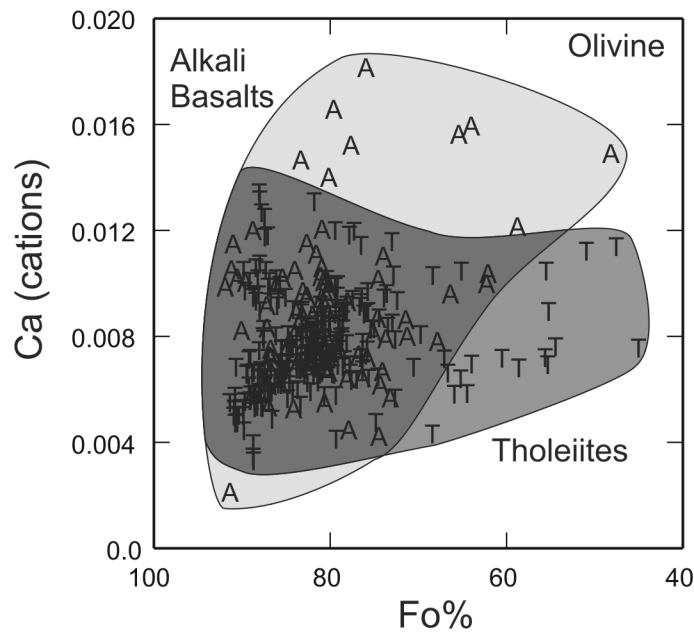


**Figure 5.** Plot of olivine forsterite content ( $Fo = 100 \cdot Mg / (Mg + Fe^{total})$ , cation proportions) versus the number of Ca cations (mineral formula based on four oxygen). As differentiation proceeds ( $Fo$  drops), Ca substitution increases in alkali basalts (A) but changes little in tholeiites (T).

gating cracks in the lithosphere (Anderson, 1999; 2000; Hamilton, 2002; 2003; see Greenough et al., in press, for a brief review of this model).

Given an internal heat source from radioactive decay, the size of the Earth, the low thermal conductivity of silicate rocks, and the temperature dependence of viscosity, mantle convec-

tion seems inevitable (Griffiths and Turner, 1998). Based on observations of the length of subduction zones, subduction and spreading rates, length and height of ocean ridges, and the topographic height of “hotspot” swells, there may be two modes of mantle convection. The dominant one is driven by cool, high-density, lithosphere sinking at

subduction zones with passive rise of mantle below spreading ocean ridges, whereas cylindrical convection cells (plumes) may be responsible for oceanic islands (Davies, 1998). Some models suggest that plumes arise from the lower most, lower mantle, thermal boundary layer (the “D” layer) heated from below by energy leaving the core. Others see cells originating at the 670 km seismic discontinuity, or from mid-mantle depths below the discontinuity (Cserepes and Yuen, 2000). It has been argued that three-dimensional views of seismic wave velocities (seismic tomography) do provide support for hot, low-density (low-velocity) diapirs (plumes) rising from the core-mantle boundary to the lithosphere below oceanic islands such as Hawaii and Iceland (Ji and Nataf, 1998; Bijwaard and Spakman, 1999; Zhao, 2001). The results of these studies and those showing subducted ocean-floor slabs crossing the upper mantle – lower mantle boundary (670 km seismic discontinuity) have recently been questioned (Anderson, 2000; Hamilton, 2003). Thus, plumes may not exist and convection in the upper mantle may be separated from the lower mantle. As discussed in the complementary paper (Greenough et al., in press), this has important implications for models of the Earth’s chemical structure and evolution.

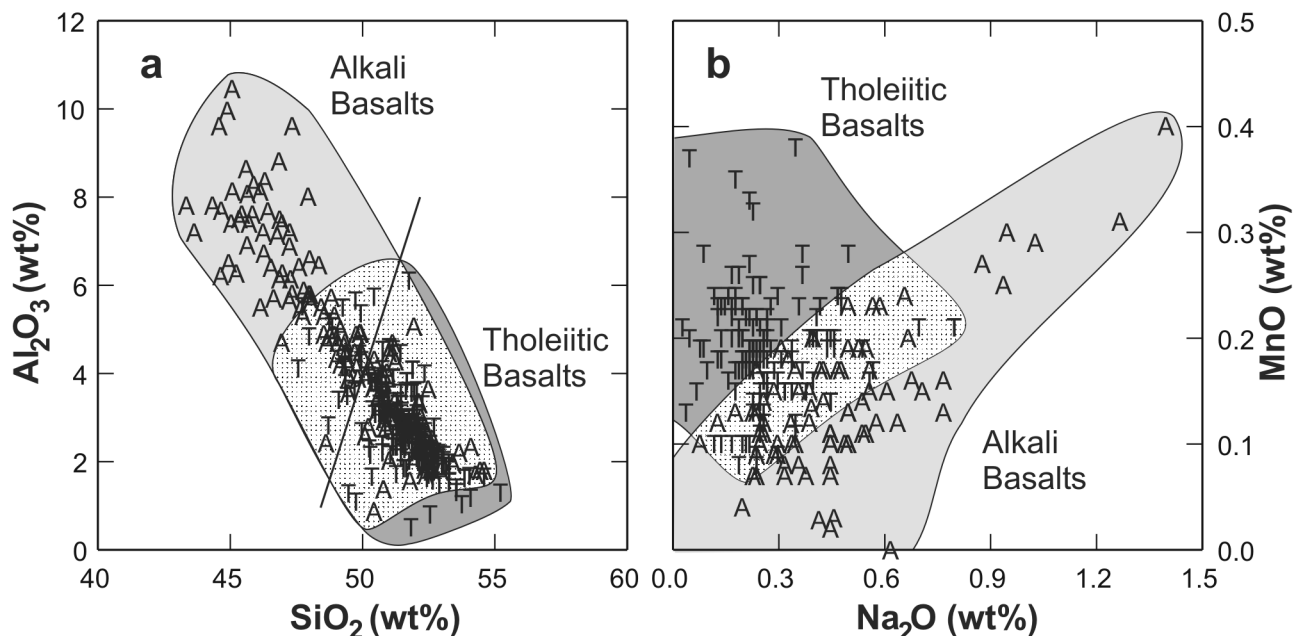


**Figure 6.** Plots showing the relationship between augite compositions and magma alkalinity. a) alkali-basalt augites (A) have higher  $Al_2O_3$  and lower  $SiO_2$  than tholeiites (T). b) The minor components MnO and  $Na_2O$  distinguish alkali and tholeiitic augites. All concentrations in oxide wt. %. The dividing line in a) is from Le Bas (1962).

Information on the magnitude of hotspot swells (0.5-1 km high \*  $\leq$  1000 km diameter), lithosphere thickness, and melting behavior of assumed mantle materials including xenoliths, yield models for the size and thermal structure of underlying convection cells. These explain changes in magma composition and volume produced by decompression melting as plates move over a hotspot (Watson and McKenzie, 1991; Sen et al., 1996). Figs. 10 and 11 show stages in Hawaiian volcanism (Clague and Dalrymple, 1987). In the pre-shield stage, the plate begins to override an ascending plume and decompression initiates melting. The initial magmas are alkaline (e.g., the subsea Loihi Seamount, southern end of the Hawaiian chain). Elements such as K, Rb, Sr, Nb, Zr, and La are highly concentrated in these incipient, small percentage melts because they are “incompatible” in minerals of the solid mantle residue and prefer melt over solid. In the second or shield stage, the plate is over the plume axis and large amounts of decompression occur. Melts form at the highest temperatures and lowest pressures resulting in large volumes of tholeiitic magma that form shield volcanoes such as Mauna Loa. “Incompatible” elements are diluted in these high-percentage melts. As the plate moves over the plume tail, melting percentages and magma production drop as alkali basalts and their differentiates appear during the post-shield stage. Following 0.3 - 2.0 Ma of dormancy with edifice erosion, small volume, explosive and highly alkaline magmas appear during a rejuvenation stage attributed to volatile-induced melting in a “wet” envelope at the plume tail’s periphery.

Lithospheric thickness determines the height to which plumes can rise (or the depth where propagating cracks initiate melting), and so it also affects the depth, volume, percentage of melting and geochemical character of magmas. After new oceanic crust forms, the lithosphere cools and thickens as it moves away from the ocean ridge. Where a plume/crack occurs below/in young and thin (< 75 km) lithosphere, low-pressure melting creates large volumes of tholeiitic magma (e.g., Iceland and Hawaii). If the lithosphere is older and thicker (e.g., Canaries) melting

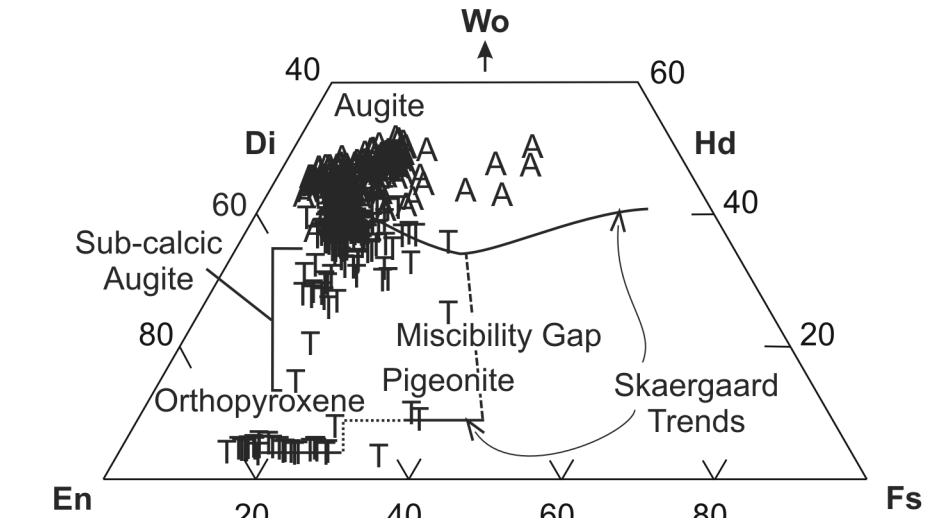


**Figure 7.** The pyroxene quadrilateral showing that alkali-basalt augites (A) have a higher wollastonite component (Wo) than those in tholeiites (T). Low-Ca pyroxenes (orthopyroxene and pigeonite) plot at the bottom of the diagram. Solid black lines show compositional trends in the tholeiitic Skaergaard Intrusion and the long-dashed line connects coexisting pyroxenes formed at ~ 1000°C. Diagram was plotted using the cation proportions of CaSiO<sub>3</sub>, MgSiO<sub>3</sub> and FeSiO<sub>3</sub>.

occurs at greater depths resulting in low volumes of dominantly alkaline magma typical of the majority of oceanic islands (Haase, 1996).

**VOLCANOLOGY AND VOLCANIC HAZARDS**

Models for the plumbing system feeding flows are mostly based on Hawaiian studies. During the shield-building stage,

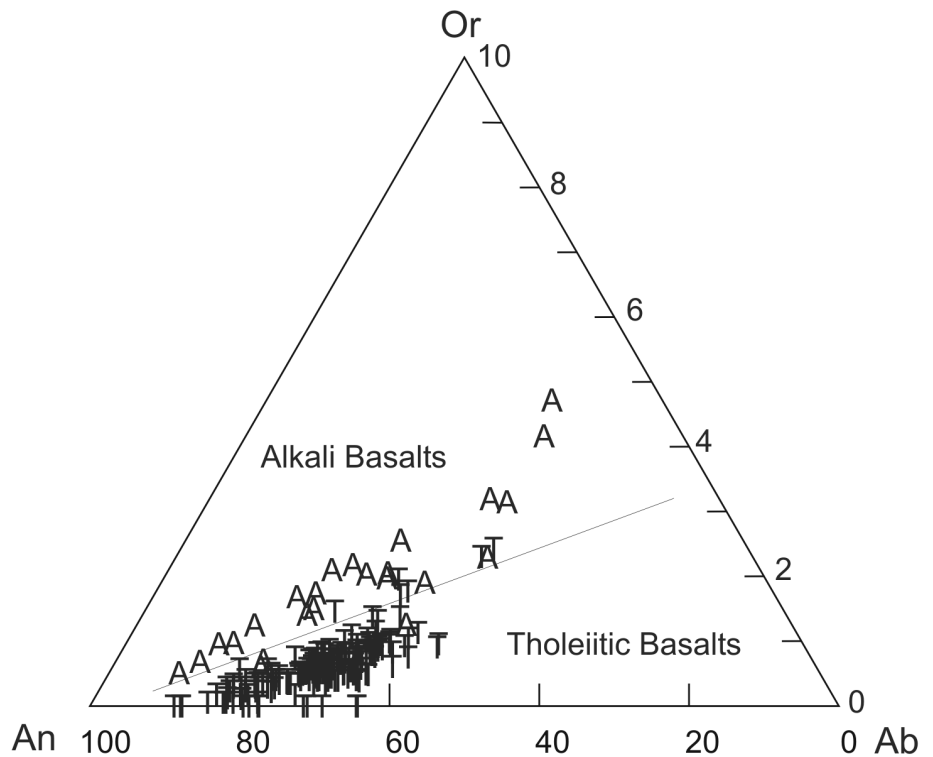


**Figure 8.** Plot of plagioclase compositions on the feldspar ternary diagram. The expanded scale for the KAlSi<sub>3</sub>O<sub>8</sub> (Or) component emphasizes the lower K content of tholeiitic plagioclases (T) compared to alkali basalts (A). Diagram was plotted using cation proportions of Ca, Na and K.

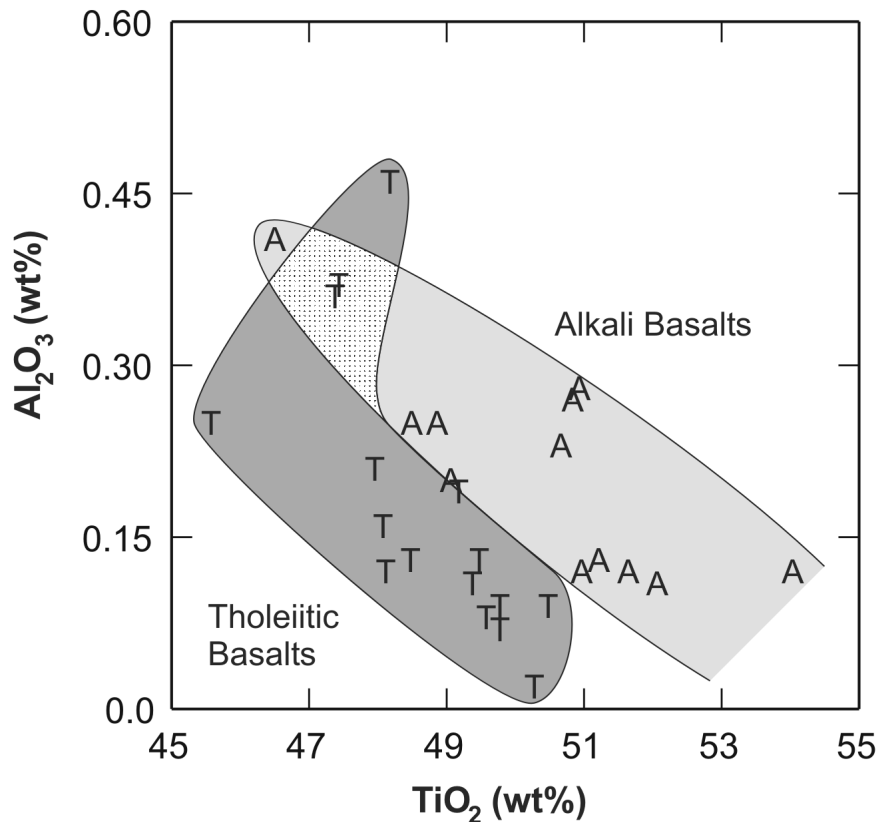


**Figure 9.** Plot of  $\text{TiO}_2$  versus  $\text{Al}_2\text{O}_3$  concentrations (oxide wt. %) in ilmenites from tholeiitic (T symbols) and alkali basalts (A). Both oxides tend to be higher in alkali basalts. See supplementary materials online at <http://www.gac.ca/JOURNALS/geocan.html> for data sources and islands represented on the plot.

magma originating from mantle depths  $\geq 60$  km penetrates a vertical conduit and is stored in a 3 to 7 km deep magma reservoir beneath the volcano's summit (Decker, 1987). During the post-shield stage, more alkalic magmas that have lower production rates are stored in deeper chambers ( $\sim 15$  km; Clague, 1987). Depending on supply rates, magma is periodically erupted from the summit and/or laterally intruded and erupted along rift zones. Rift zone orientations reflect the gravity-induced tensional stress field that is controlled by a volcano's internal structure and morphology (Fiske and Jackson, 1972). The volume (0.08 to 40  $\text{km}^3$ ) and shape (interconnected sills and dykes versus spherical pluton) of magma chambers below Kilauea are debated but temporal geochemical variations suggest a small (2-3  $\text{km}^3$ ), simple-shaped reservoir, whereas geophysical models "see" a large aseismic zone (chamber) that includes crystal mush (Pietruszka and Garcia, 1999).

The relatively non-explosive

eruption of copious quantities of high-temperature, low-viscosity (highly fluid) basaltic lava results in the low slopes characterizing shield volcanoes. High temperature pahoehoe flows near vents have smooth "ropey" surfaces (Williams and McBirney, 1979, pp. 101-112).

Lower temperature flows, and flows farther from vents are more viscous and have uneven, jagged or broken surfaces (aa and blocky flows). Pillow lavas form where lava is extruded under water. The outer selvages are glassy and the interior tends to be vesicular under low-water pressures. At great ocean depths (pressure), lower magma volatile contents, and/or higher magma viscosities, pillow interiors are less vesicular. Evolved (differentiated) and alkaline magmas tend to be more explosive reflecting higher viscosity and/or higher volatile content. Thus, post-shield and rejuvenation-stage alkaline magmas are more prone to forming localized, cone-shaped, fragmental deposits (Mullineaux et al., 1987). Magma interaction with groundwater or seawater, either before or in association

with eruption, enhances the formation of fragmental rocks (Cas and Wright, 1987, pp. 42-45).

Non-explosive shield volcano eruptions rarely result in human deaths but lava flows, the most common type of volcanic hazard (e.g., Hawaii), can be very destructive (Mullineaux et al., 1987). More daunting is the tendency for oceanic islands to undergo catastrophic collapse. The seafloor surrounding most oceanic islands shows debris-flow deposits stretching hundreds of kilometres from islands (e.g., Moore et al., 1994; McMurtry et al., 1999; Moore and Clague, 2002). Various factors contribute to the collapse (Elsworth and Voigt, 1996; Carracedo, 1996). These are: 1) flows extruded into seawater become quenched and contribute to over-steepening of the volcanic edifice. The result is a tensional stress regime, induced by gravity, which radiates from volcano summits, 2) porous subaerial fragmental deposits can be intruded by impermeable dykes. In humid climates the porous rocks between sub-parallel dykes in rift zones become saturated water reservoirs, and 3) intrusion along rift zones facilitates catastrophic collapse because magma has no shear or tensional strength and it also decreases the strength of surrounding rocks by heating trapped water and raising pore-fluid pressures. The potential for catastrophic collapse has attracted much attention because resulting giant tsunamis could imperil major cities bordering the ocean basins.

## GEOCHEMISTRY AND DIFFERENTIATION

Once magmas form in the mantle, various processes, including differentiation, can cause them to evolve. The products of these various processes are highly dependent on the starting magma composition. Basalts and rarer intermediate and felsic rocks can be categorized into three series based on  $\text{Na}_2\text{O} + \text{K}_2\text{O}$  at particular  $\text{SiO}_2$  contents (Fig. 12a; averages used appear in supplementary materials with representative averages in Greenough et al. (in press; their Table 1). Three reference suites from Iceland, Moorea and Tristan da Cunha illustrate (respectively) the tholeiitic series containing basalt to rhyolite, the alkaline series with alkali basalts to trachytes and a strongly alkaline series, beginning with

basanite and ultimately yielding phonolite; few oceanic islands contain tholeiite-series rocks. The alkaline series is most common (Fig. 12b). Variations in composition within each series reflect differentiation in magma chambers under volcanoes. Crystals (minerals) have a different bulk composition than the magma they form from. For example, early crystallizing olivine has higher MgO, lower SiO<sub>2</sub> and little Na<sub>2</sub>O and K<sub>2</sub>O compared to the host magma. Its formation causes the residual liquid (magma) to have lower MgO and higher SiO<sub>2</sub> and Na<sub>2</sub>O + K<sub>2</sub>O content than the original magma. Magma chambers are not exposed, so processes that remove crystals from magma must be inferred from erupted flows. Whether minerals grow in magma and are gravitationally separated (i.e., minerals denser than magma, sink), or nucleate and grow on the floor, walls and roof of chambers from convecting magma, is debated (see Hawkesworth et al., 2000) but most petrologists are of the view that crystal fractionation, in whatever form, is the dominant differentiation process. Intermediate composition lavas tend to be less common, or missing, in some suites, a phenomenon called the Daly gap. The Daly gap has been related to high viscosities (Thompson et al., 2001) and/or higher densities (Renzulli and Santi, 2000) of intermediate magmas, which prevent them from reaching the surface. Evolved magmas can have lower viscosities than intermediate ones because of increased alkalis and volatile contents. This, together with volatile exsolution, which creates buoyant magma, allows evolved magma to erupt.

Various approaches yield information about how magmas evolve. For example, olivine is a common phenocryst phase in both Kilauea and Mauna Loa tholeiites. The effect of olivine formation and removal on magma composition can be calculated, and matches glass compositions observed at both volcanoes. Projection of these liquid compositions onto experimentally determined phase diagrams reveals that the slightly higher silica content of Mauna Loa magmas causes evolving liquids to intersect the olivine - pyroxene cotectic. Therefore, pyroxene is the next mineral to start forming after olivine. Plagioclase comes onto the liquidus after pyroxene. In contrast, olivine

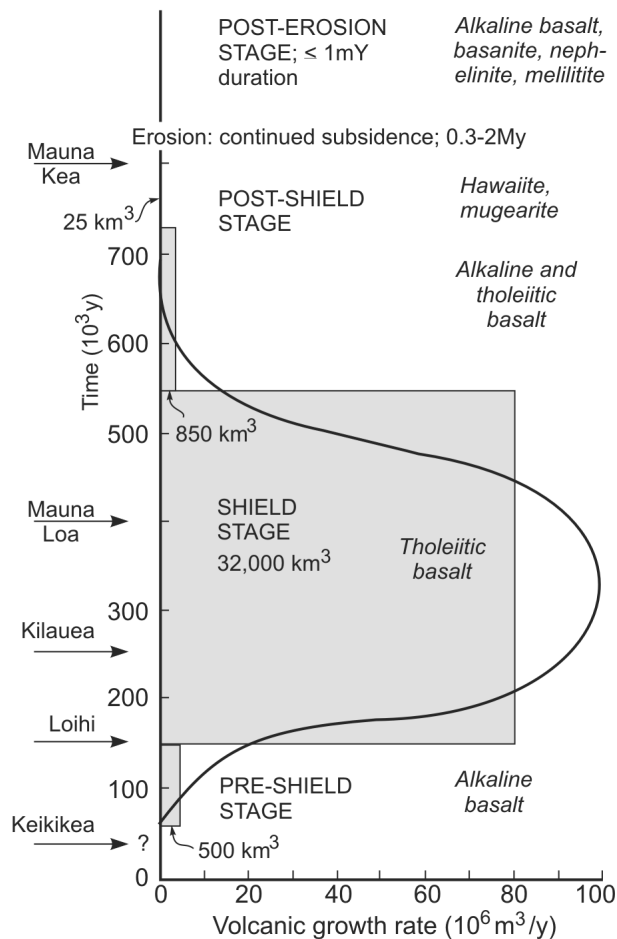


**Figure 10.** Graphical representation of time (Y axis) versus magma eruption rates (solid curve; X axis), accumulated volume (shaded rectangles) and rock types (right hand column) for Hawaiian volcanoes at various stages of development. Example volcanoes are given on the Y axis. Note that percentages of melting correlate positively with the eruption rates represented by the bell-shaped curve. Modified from Best and Christiansen (2001, p. 359).

formation and removal causes Kilauea magmas to intersect the olivine - plagioclase cotectic. Thus the order of phenocryst appearance in Kilauea lavas is olivine, plagioclase, augite whereas in Mauna Loa lavas it is olivine, augite, plagioclase (Basaltic Volcanism Study Project, 1981, p. 165).

Mass-balance calculations and trace-element modeling are widely used to infer how magmas evolve (e.g., Maaløe et al. 1986; West et al., 1988; Le Roex, 1990; Thompson et al., 2001). Generalizations on processes can be made from variation diagrams showing representatives of the three magma series (Fig. 13). Selected major elements and trace elements are plotted against Mg# (= Mg/(Mg + (0.9\*Fe<sup>total</sup>)) atomic) which decreases during differentiation reflecting the preferential incorporation of Mg over Fe in ferromagnesian miner-

als. Nickel, Cr and Co behave as “compatible” elements (i.e., are concentrated in early crystallizing minerals) in all three series with the concentrations falling as Mg# declines. Declining Ni and Co are most commonly ascribed to olivine precipitation. However, globules of high-density, immiscible sulfide liquid can also form in the early stages of magma differentiation. Sulfide liquid removes Ni more rapidly than olivine because of the extremely high-sulfide liquid/silicate magma partitioning coefficients. Some siderophile and chalcophile elements such as Au and the Platinum Group elements (PGE’s) are more strongly partitioned into immiscible sulfide liquid than Ni. Thus, the removal of sulfide liquid may explain the compatible behavior (concentrations fall with differentiation) of these elements in many hot-spot magmas (Fryer and Greenough, 1992;

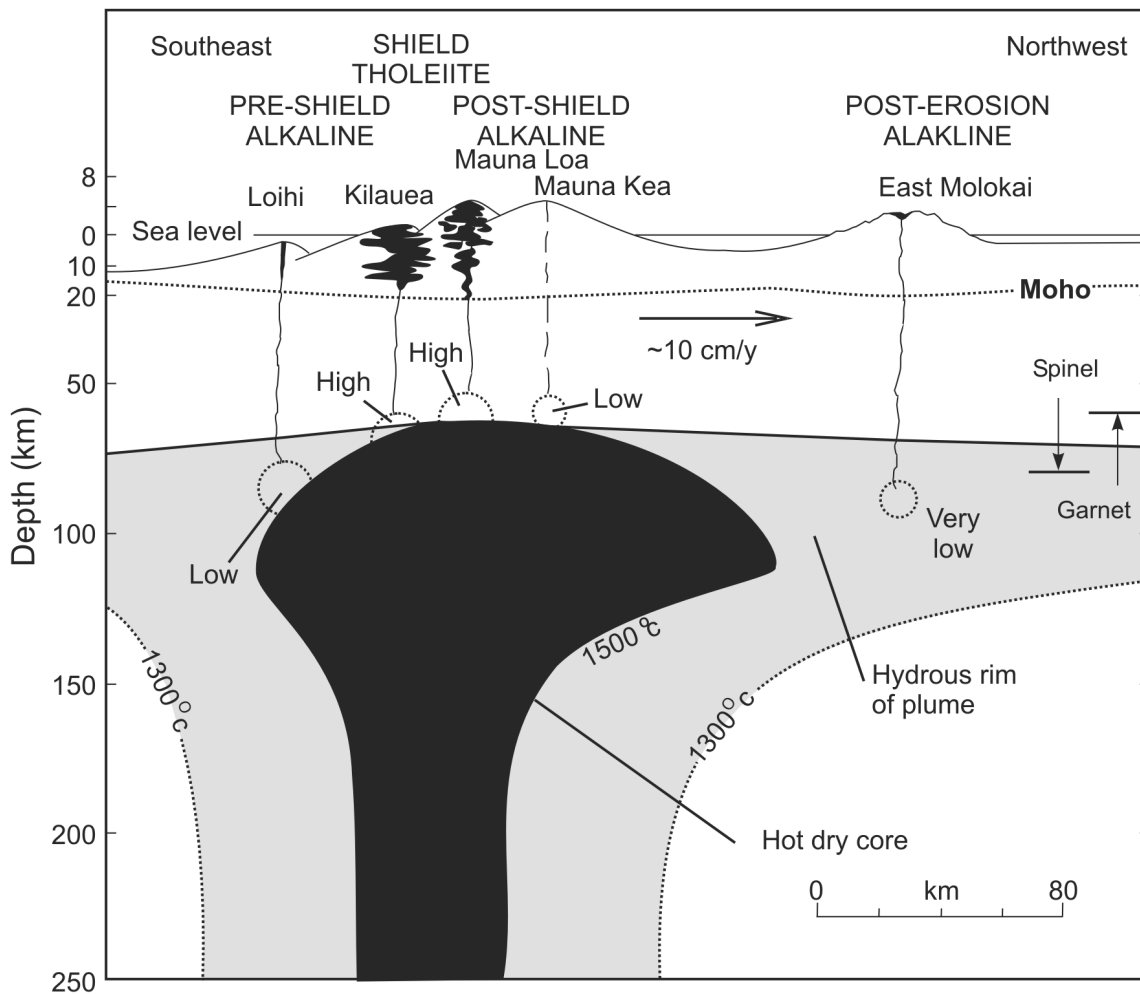


**Figure 11.** Schematic cross section along the axis of the Hawaiian island chain showing relationships between the underlying plume and volcanoes at various stages of development. Circles give the volume and percentage of melting (high, low, etc.) at each volcano. Temperature contours outline the plume's shape which is asymmetric reflecting viscous drag from the moving, overlying lithosphere. Alkaline magmas form at the rim of the plume, which is hydrated by metasomatic fluids driven from the hot dry (dehydrated) core. Scales on the X and Y axes are the same except that the above-sea-level part of Y is expanded to show surface features. Modified from Best and Christiansen (2001, p. 362) and Sen et al. (1996).

Tatsumi et al., 2000). Chromium decreases are commonly attributed to the early precipitation of chromite, and later, the formation of augite.

Strontium tends to increase in basalts and then plunge in more differentiated rocks ( $Mg\# > 0.40$ ) of alkaline and strongly alkaline islands, (e.g., Tristan da Cunha, Fig. 13); plagioclase concentrates Sr. The change from incompatible to compatible behavior heralds the onset of significant plagioclase (or feldspathoid) precipitation/removal. Similarly, Ba behaves incompatibly in mafic magmas but concentrations either level off or fall in highly differentiated rocks. Declining Rb and Ba in evolving, alkaline Hawaiian rocks has been ascribed to feldspar precipitation (West et al., 1988) because

both elements have high partition coefficients in K-feldspars (e.g., sanidine).

The rare-earth-elements (except Eu), and high-field strength elements (e.g., Zr, Hf, Nb, Ta) generally behave incompatibly (Fig. 13). However, Nb and Ta are compatible in some Jan Mayen and Hawaiian suites, apparently reflecting Fe-Ti oxide precipitation (Maaløe et al., 1986; West et al., 1988). Phosphorous initially rises and then falls in Tristan da Cunha lavas, but remains constant, or falls, in the Moorea and Iceland suites (Fig. 13). Although P can be incompatible in entire suites (West et al., 1988), apatite comes on the liquidus by intermediate to late stages of differentiation in many suites as indicated by declining P concentrations (e.g., Thompson et al., 2001; Maaløe et al.,

1986). Note that because the REE partition into apatite, the proportion of apatite precipitating must be large enough to remove P but small enough to keep the bulk partition coefficient for the REE less than one because their concentrations increase with differentiation. Titanium may initially increase during differentiation, but it becomes compatible in all types of magmas above an  $Mg\#$  of  $\sim 0.5$  (Fig. 13). Minerals that remove Ti include augite and ilmenite/titanomagnetite.

An important question is whether the alkaline and tholeiitic series magmas are related by differentiation. Classic experiments by Yoder and Tilley in the 1960's showed that Ne-normative alkali basalts are probably not related to tholeiitic basalts by differentiation

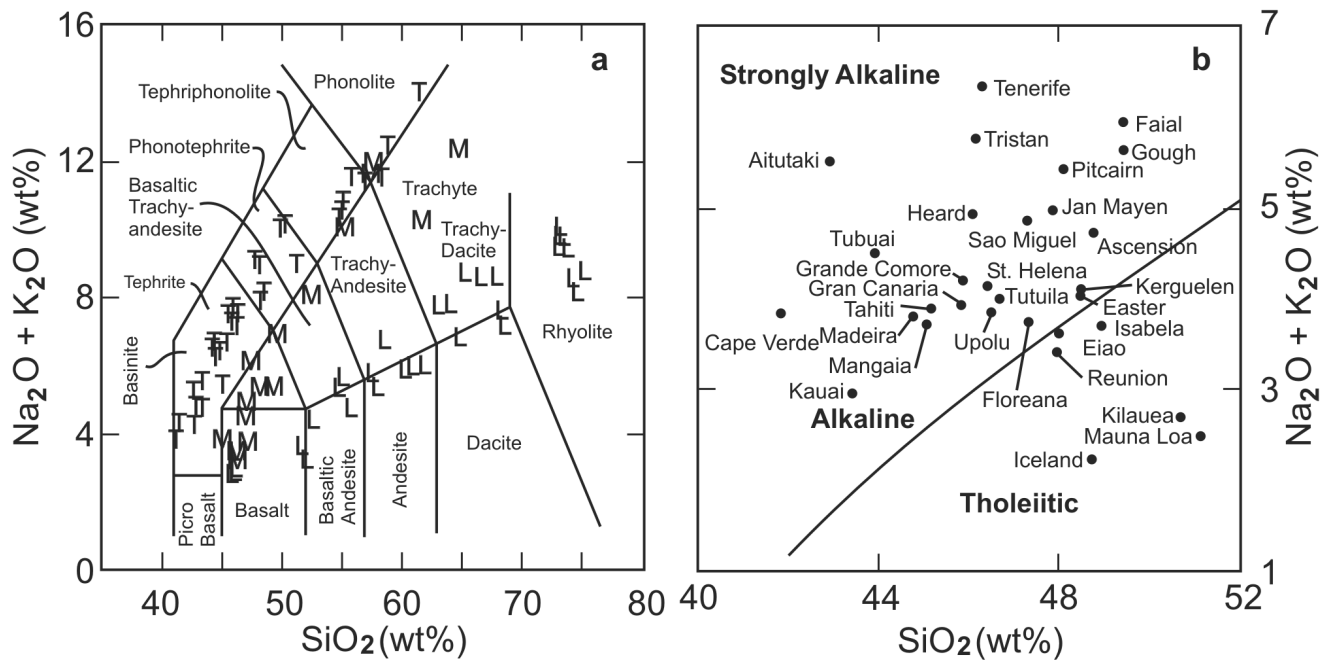


**Figure 12.** Total alkalis versus silica diagrams. a) Suites of differentiated rocks from Tristan da Cunha (T), Moorea (Society Islands, M) and Iceland (L). Fields are from Le Maitre et al., (1989) b) Averaged compositions of basalts from 30 oceanic islands as labelled. The dividing line for alkaline and tholeiitic (subalkaline) fields is from Irvine and Baragar (1971). Averages used for diagram b) appear in the supplementary materials with selected representative analyses in Greenough et al. (in press).

because of a low-pressure thermal divide approximately coinciding with the Ol - Ab join in the basalt tetrahedron (Fig. 3). To cross this divide, basaltic magmas would have to increase in temperature as they differentiate (see Petrography and Mineralogy Section). Both series show similar maximum Mg# values and concentrations of differentiation-sensitive transition metals (Ni, Cr, Co, Sc). This precludes fractional crystallization even at high pressures as a process relating the two types of basalts (Dostal et al., 1982). However, Renzulli and Santi (2000) show that under high fO<sub>2</sub> conditions, slightly Ne-normative basalts can yield highly evolved peralkaline, Hy- and Q-normative trachytes through a two-stage fractionation process occurring in deep and then shallow-level magma chambers.

**Assimilation**

Although fractional crystallization is seen as the dominant process yielding highly evolved rocks (e.g., Prestvik et al., 2001), other magma chamber processes can be important. The phase change associated with crystallization releases large amounts of energy that is converted to heat; this heat causes melting or partial melting of wall rocks, a process called assimilation – fractional crystal-

lization (AFC). For example, high <sup>87</sup>Sr/<sup>86</sup>Sr ratios in Kerguelen trachytes supports assimilation of hydrothermally altered oceanic crust in subsurface magma chambers (Gagnevin et al., 2003). However, even basalts can be contaminated. The K<sub>2</sub>O and P<sub>2</sub>O<sub>5</sub> concentrations, and <sup>206</sup>Pb/<sup>204</sup>Pb and <sup>143</sup>Nd/<sup>144</sup>Nd isotopic compositions of melt, fluid and crystal inclusions in olivine from a relatively unevolved Kerguelen basalt, indicate assimilation of the underlying lithosphere (Borisova et al., 2002). Oxygen isotopes (δ<sup>18</sup>O) are useful for identifying contaminants such as altered basalt and seafloor sediment. Variations in the δ<sup>18</sup>O of Canary islands phonolites and basalts, as well as Icelandic basalts, support assimilation of felsic rocks (e.g., nepheline syenite) from the volcanic edifice (Wolff et al., 2000), ocean floor, and island crustal rocks (Hansteen and Troll, 2003; Eiler et al., 2000). Studies of volatiles (e.g., H<sub>2</sub>O, CO<sub>2</sub>, Cl, F, S, B, Be), in particular Cl, in Hawaiian and Austral Islands basaltic glass and olivine-hosted melt inclusions suggest that intruding magmas commonly assimilate subsurface seawater, hydrothermal brines or brine-impregnated oceanic crust, and fumarolic deposits (Lassiter et al., 2002; Hauri, 2002; Davis et al., 2003).

**Time scales of Differentiation**

Uranium-series dating (Hawkesworth et al., 2000; Condomines et al., 2003; Reid, 2003) has been important for estimating differentiation time-scales in closed-system magma chambers, and magma residence times for open systems (magma constantly erupting; e.g., Kilauea, Hawaii). Uranium-series methods are based on the concept of radioactive equilibrium. In an “old” system (e.g., old mineral grain) the number of daughter atoms forming per unit time from parent atoms (referred to as Activity of the parent = (A<sub>p</sub>)) will equal the number of daughters decaying to some other isotope (Activity of daughter = (A<sub>D</sub>)) and (A<sub>D</sub>/A<sub>p</sub>) = 1. Young systems can be in a state of disequilibrium; the number of daughter atoms forming (or decaying) is greater than the number decaying (or forming). The extent to which the system is out of equilibrium reflects how young it is. The U and Th decay series that lead to stable Pb isotopes involve numerous intermediate isotopes with short half-lives. The commonly used parent–daughter pairs <sup>238</sup>U – <sup>230</sup>Th, <sup>235</sup>U – <sup>231</sup>Pa, <sup>230</sup>Th – <sup>226</sup>Ra, <sup>226</sup>Ra – <sup>210</sup>Pb and <sup>232</sup>Th – <sup>228</sup>Ra (daughter 1/2 lives = 75400, 32500, 1620, 22.3 and 5.75 years respectively) permit “dating” on time scales of ~400,000 years to a few years

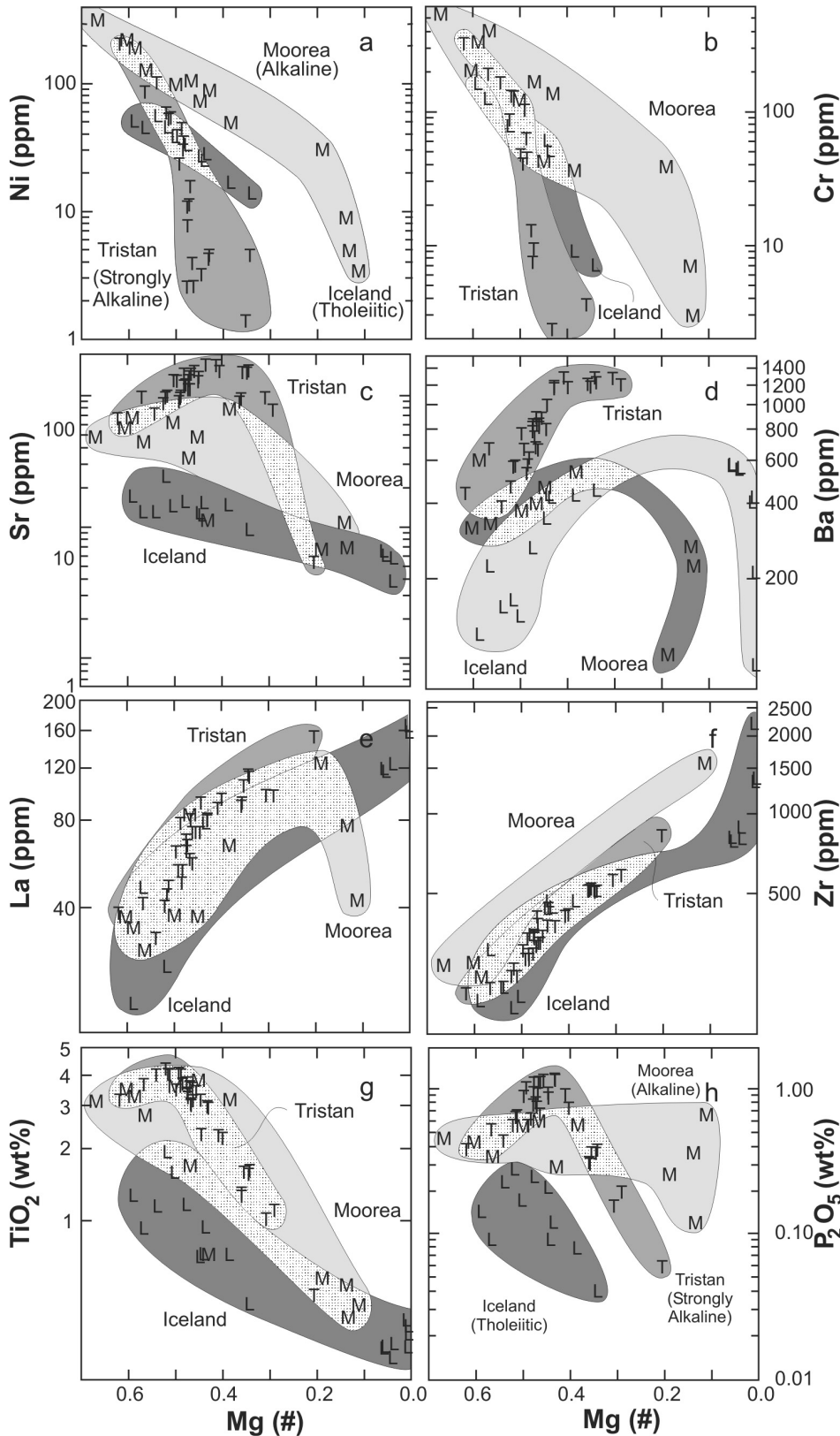


**Figure 13.** Plots of selected trace elements (ppm) and major element oxides (wt. %) versus the differentiation indicator  $Mg\#$  ( $= Mg/(Mg + (0.9 \cdot Fe^{\text{total}}))$  atomic) in three suites of oceanic island basalts. Tristan da Cunha (T) represents a strongly alkaline suite, Moorea Society Islands, (M) a moderately alkaline suite and Iceland (L) a tholeiitic suite. Note concentrations on the Y axis are on a log scale.

( $\sim 5$  times  $1/2$  lives). Based on  $^{238}U - ^{230}Th$ , differentiation of alkali basalt to form trachyte in deep magma chambers (e.g., Sao Miguel, Azores; Tenerife, Canarys) takes  $\sim 10^5$  years, although these could be an over-estimate if old crustal materials were assimilated (Condomines et al., 2003).  $^{226}Ra - ^{210}Pb$  methods indicated only  $\sim 10$  years were required for alkali basalt to differentiate to hawaiite/mugearite in Iceland (Sigmarsson, 1996). For “open systems”, a  $^{230}Th - ^{226}Ra$  study of an evolved Kilauea rift basalt gave a minimum residence time of  $\sim 550$  years (Cooper et al., 2001). Reid (2003) states that  $^{230}Th - ^{226}Ra$  disequilibria indicate residence times of, at most, a few thousand years and more commonly years to hundreds of years.

#### Differentiation in Flows

Rapid (years to 10's of years) differentiation processes occur in individual basaltic flows and form igneous layering with “exotic” compositions. Segregation veins create the layering. They occur in basalt flows  $> 10$ -m thick, are 1 - 100-cm thick, vertical to horizontal (=sheets; traceable 100's of m) and show sharp, but unchilled boundaries with surrounding basalt. Textures change from highly vesicular (upper 5 m), to pegmatitic at depths of  $\sim 30$  m (Greenough et al., 1999). As the flow's upper crust grows downward, horizontal segregation veins form at regular intervals reflecting tearing of crystal mush at the bottom of the crust (Helz, 1987). Interstitial liquid in the mush is sucked or forced into the tear to produce the vein. Convection contributes to the exotic compositions of segregation veins (Helz et al., 1989). Various processes can cause low-density residual magma to form at the bottom of the flow. This magma forms diapirs or vesicle “plumes” (not mantle plumes!) that rise through the flow, infiltrate the crystal mush of the flow's upper crust, and ultimately enter segregation veins. Veins show high concentrations of elements likely to form volatile complexes (K, Na, Rb, Sr, Ba, Cu, Pb, Zn, Cl, S and As) implicating volatiles and vesicle “plumes” in the differentiation process (Greenough et al., 1999). Similar rapid differentiation processes may operate in subsurface magma chambers.

## FUTURE RESEARCH

The issue of whether oceanic islands form from mantle plumes or represent propagating cracks in the lithosphere is of fundamental importance and requires a re-evaluation of seismic tomography results. Although the importance of crystal differentiation appears established, the impact of assimilation and effect of volatiles on magma compositions requires further consideration. Studies of the trace-element composition of minerals using new analytical methods such as laser ablation – inductively-coupled-plasma mass-spectrometry, promise refinements in our understanding of differentiation processes as well as alternative methods for assessing relationships between magma chemistry and source region processes and compositions.

## ACKNOWLEDGEMENTS

R. Corney prepared diagrams. SMU provided office support for LMM and JDG. JDG and JD acknowledge NSERC operating grants. The comments of reviewers (G. Jenner, B. Murphy and D. Piper) and the editor (G. Pe-Piper) led to major improvements in the manuscript.

## SUPPLEMENTARY MATERIAL

Supplementary material, which includes a table listing average data for selected oceanic islands, plus data selection procedures and an extensive list of references, can be viewed at the following location: <http://www.gac.ca/JOURNALS/geocan.html>.

## REFERENCES

- Allègre, C.J., 2002, The evolution of mantle mixing: *Philosophical Transactions of the Royal Society of London A*, v. 360, p. 2411-2431.
- Andersen, D.J. and Lindsley, D.H., 1988, Internally consistent solution models for Fe-Mg-Mn-Ti oxides; Fe-Ti oxides: *American Mineralogist*, v. 73, p. 714-726.
- Anderson, D.L., 1999, A theory of the Earth; Hutton and Humpty Dumpty and Holmes, *in* Craig, G.Y. and Hull, J.H., eds., *James Hutton; present and future*: Geological Society Special Publications, v. 150, p. 13-35.
- Anderson, D.L., 2000, The thermal state of the upper mantle; no role for mantle plumes: *Geophysical Research Letters*, v. 27, p. 3623-3626.
- Basaltic Volcanism Study Project, 1981, *Basaltic Volcanism on the Terrestrial Planets*: Pergamon Press Inc., New York, 1286 pp.
- Best, M.G. and Christiansen, E.H., 2001, *Igneous Petrology*. Blackwell Science, Massachusetts, 458 p.
- Bijwaard, H. and Spakman, W., 1999, Tomographic evidence for a narrow whole mantle plume below Iceland: *Earth and Planetary Science Letters*, v. 166, p. 121-126.
- Borisova, A.Y., Nikogosian, I.K., Scoates, J.S., Weis, D., Damasceno, D., Shimizu, N. and Touret, J.L.R. 2002, Melt, fluid and crystal inclusions in olivine phenocrysts from Kerguelen plume-derived picritic basalts; evidence for interaction with the Kerguelen Plateau lithosphere: *Chemical Geology*, v. 183, p. 195-220.
- Carracedo, J.C., 1996, A simple model for the genesis of large gravitational landslide hazards in the Canary Islands, *in* McGuire, W.J., Jones, A.P. and Neuberg, J. eds., *Volcano Instability on the Earth and Other Planets*: Geological Society Special Publication No. 110, Geological Society, Bath, U.K., p. 125-135.
- Cas, R.A.F. and Wright, J.V., 1987, *Volcanic Successions, Modern and Ancient*. Allen and Unwin, London, 528 p.
- Clague, D.A., 1987, Hawaiian alkaline volcanism, *in* Fitton, J.G. and Upton, B.G.J., eds., *Alkaline Igneous Rocks*: Geological Society Special Publication No. 30, p. 227-252.
- Clague, D.A. and Dalrymple, G.B., 1987, The Hawaii-Emperor volcanic chain, Part I, geologic evolution, *in* Decker, R.W., Wright, T.L. and Stauffer, P.H., eds., *Volcanism in Hawaii*, Volume 1: U.S. Geological Survey Professional Paper 1350, p. 5-54.
- Condomines, M., Gauthier, P.-J. and Sigmarrsson, O., 2003, Timescales of magma chamber processes and dating of young volcanic rocks, *in* Bourdon, B., Henderson, G.M., Lundstrom, C.C. and Turner, S.P., eds., *Uranium-series geochemistry: Reviews in Mineralogy and Geochemistry*, v. 52, p. 125-174.
- Cooper, K.M., Reid, M.R., Murrell, M.T. and Clague, D.A., 2001, Crystal and magma residence at Kilauea Volcano, Hawaii;  $^{230}\text{Th}$ - $^{226}\text{Ra}$  dating of the 1955 East Rift eruption: *Earth and Planetary Science Letters*, v. 184, p. 703-718.
- Crough, S.T., 1983, Hotspot swells: Annual Review of Earth and Planetary Sciences, v. 11, p. 165-193.
- Cserepes, L. and Yuen, D.A., 2000, On the possibility of a second kind of mantle plume: *Earth and Planetary Science Letters*, v. 183, p. 61-71.
- Davidson, P.M. and Lindsley, D.H., 1985, Thermodynamic analysis of quadrilateral pyroxenes; Part 2, Model calibration from experiments and applications to geothermometry: *Contributions to Mineralogy and Petrology*, v. 91, p. 390-404.
- Davies, G.F., 1998, Plates, plumes, mantle convection and mantle evolution, *in* Jackson, I., ed., *The Earth's Mantle, Composition, Structure and Evolution*: Cambridge University Press, Cambridge, U.K., p. 228-258.
- Davis, M.G., Garcia, M.O. and Wallace, P., 2003, Volatiles in glasses from Mauna Loa Volcano, Hawaii; implications for magma degassing and contamination, and growth of Hawaiian volcanoes: *Contributions to Mineralogy and Petrology*, v. 144, p. 570-591.
- Decker, R.W., 1987, Dynamics of Hawaiian volcanoes: an overview, *in* Decker, R.W., Wright, T.L. and Stauffer, P.H., eds., *Volcanism in Hawaii*: U.S. Geological Survey Professional Paper 1350, v. 2, p. 997-1018.
- Dostal, J., Dupuy, C. and Liotard, J.M., 1982, Geochemistry and origin of basaltic lavas from Society Islands, French Polynesia (South Central Pacific Ocean): *Bulletin of Volcanology*, v. 45, p. 51-62.
- Duncan, R.A. and Richards, M.A., 1991, Hotspots, mantle plumes, flood basalts, and true polar wander: *Reviews of Geophysics*, v. 29, p. 3150.
- Eiler, J.M., Grövdal, K. and Kitchen, N., 2000, Oxygen isotope evidence for the origin of chemical variations in lavas from Theistareykir Volcano in Iceland's northern volcanic zone: *Earth and Planetary Science Letters*, v. 184, p. 269-286.
- Elsworth, D. and Voigt, B., 1996, Evaluation of volcano flank instability triggered by dyke intrusion, *in* McGuire, W.J., Jones, A.P. and Neuberg, J., eds., *Volcano Instability on the Earth and Other Planets*: Geological Society Special Publication No. 110, Geological Society, Bath, U.K., p. 45-53.
- Fiske, R.S. and Jackson, E.D., 1972, Orientation and growth of Hawaiian volcanic rifts: the effect of regional structure and gravitational stresses: *Proceedings of the Royal Society of London, Series A*, v. 329, p. 299-326.
- Fryer, B.J. and Greenough, J.D., 1992, Evidence for mantle heterogeneity from platinum-group-element abundances in Indian Ocean basalts: *Canadian Journal of Earth Sciences*, v. 29, p. 2329-2340.
- Gagnevin, D., Ethien, R., Bonin, B., Moine, B., Feraud, G., Gerbe, M.C., Cottin, J.Y., Michon, G., Tourpin, S., Mamias, G., Perrache, C. and Giret, A., 2003, Open-system processes in the genesis of silica-oversaturated alkaline rocks of the



- Rallier-du-Baty Peninsula, Kerguelen Archipelago (Indian Ocean): *Journal of Volcanology and Geothermal Research*, v. 123, p. 267-300.
- Greenough, J.D., Dostal, J. and Mallory-Greenough, L.M., 2005. Oceanic Island Volcanism II: Mantle Processes. *Geoscience Canada*, v. 32, number 2, in press.
- Greenough, J.D., Lee, C.-Y. and Fryer, B.J., 1999, Evidence for volatile-influenced differentiation in a layered alkali basalt flow, Penghu Islands, Taiwan: *Bulletin of Volcanology*, v. 60, p. 412-424.
- Griffiths, R.W. and Turner, J.S., 1998, Understanding mantle dynamics through mathematical models and laboratory experiments, *in* Jackson, I., ed., *The Earth's Mantle: Composition, Structure, and Evolution*: Cambridge University Press, Cambridge, U.K., p. 191-227.
- Haase, K.M., 1996, The relationship between the age of the lithosphere and the composition of oceanic magmas: constraints on partial melting, mantle sources and the thermal structure of the plates: *Earth and Planetary Science Letters*, v. 144, p. 75-92.
- Hamilton, W.B., 2002, The closed upper-mantle circulation of plate tectonics: *American Geophysical Union Geodynamics Series*, v. 30, p. 359-410.
- Hamilton, W.B., 2003, An alternative Earth: *GSA Today*, v. 13, p. 4-12.
- Hansteen, T.H. and Troll, V.R. 2003, Oxygen isotope composition of xenoliths from the oceanic crust and volcanic edifice beneath Gran Canaria (Canary Islands); consequences for crustal contamination of ascending magmas: *Chemical Geology*, v. 193, p.181-193.
- Hauri, E., 2002, SIMS analysis of volatiles in silicate glasses, 2: isotopes and abundances in Hawaii melt inclusions: *Chemical Geology*, v. 183, pp. 115-141.
- Hawkesworth, C.J., Blake, S., Evans, P., Hughes, R., MacDonald, R., Thomas, L.E., Turner, S.P. and Zellmer, G., 2000, Time scales of crystal fractionation in magma chambers; integrating physical, isotopic and geochemical perspectives: *Journal of Petrology*, v. 41, p. 991-1006.
- Helz, R.T., 1987, Differentiation behaviour of Kilauea Iki lava lake, Kilauea Volcano, Hawaii: an overview of past and current work: *Geochemical Society, Special Publication 1*, p. 241-258.
- Helz R.T., Kirschenbaum H. and Marinenko J.W., 1989, Diapiric transfer of melt in Kilauea Iki lava Lake, Hawaii: a quick, efficient process of igneous differentiation: *Geological Society of America Bulletin*, v. 101, p. 578-594.
- Hughes, C.J., 1982, *Igneous Petrology*: Elsevier Scientific Publishing Co., New York, 551 p.
- Irvine, T.N. and Baragar, W.R.A., 1971, A guide to the chemical classification of the common volcanic rocks: *Canadian Journal of Earth Sciences*, v. 8, p. 523-548.
- Ji, Y. and Nataf, H.C., 1998, Detection of mantle plumes in the lower mantle by diffraction tomography: Hawaii: *Earth and Planetary Science Letters*, v. 159, p. 99-115.
- Koppers, A.A.P., Morgan, J.P., Morgan, J.W. and Staudigel, H., 2001, Testing the fixed hotspot hypothesis using  $^{40}\text{Ar}/^{39}\text{Ar}$  age progressions along seamount trails: *Earth and Planetary Science Letters*, v. 185, p. 237-252.
- Lassiter, J.C., Hauri, E.H., Nikogosian, I.K. and Barszczus, H.G., 2002, Chlorine-potassium variations in melt inclusions from Raivavae and Rapa, Austral Islands; constraints on chlorine recycling in the mantle and evidence for brine-induced melting of oceanic crust: *Earth and Planetary Science Letters*, v. 202, p. 525-540.
- Le Bas, M.J., 1962, The role of Aluminum in igneous clinopyroxenes with relation to their parentage: *American Journal of Science*, v. 260, p. 267-288.
- Le Maitre, R. W. [ed]; Bateman, P.; Dudek, A.; Keller, J.; Lemeyre, J.; Le Bas, M. J.; Sabine, P. A.; Schmid, R.; Sorensen, H.; Streckeisen, A.; Wooley, A. R.; and Zanettin, B., 1989, *A classification of igneous rocks and glossary of terms*: Blackwell Scientific, Oxford, United Kingdom, 193 p.
- Le Roex, A.P., Cliff, R.A. and Adair, B.J.I., 1990, Tristan da Cunha, South Atlantic; geochemistry and petrogenesis of a basanite-phonolite lava series: *Journal of Petrology*, v. 31, p. 779-812
- Maaløe, S., Sørensen, I. and Hertogen, J., 1986, The trachybasaltic suite of Jan Mayen: *Journal of Petrology*, v. 27, p. 439-466.
- Mallory-Greenough, L.M., Gorton, M.P. and Greenough, J.D., 2002, The source of basalt vessels in ancient Egyptian archaeological sites: a mineralogical approach: *Canadian Mineralogist*, v. 40, p. 1025-1046.
- McGuire, W.J., 1996, Volcano instability: a review of contemporary themes, *in* McGuire, W.J., Jones, A.P. and Neuberg, J., eds., *Volcano Instability on the Earth and Other Planets*: Geological Society Special Publication No. 110, Geological Society, London, p. 1-23.
- McMurtry, G.M., Herrero-Bervera, E., Cremer, M.D.; Smith, J.R., Resig, J., Sherman, C. and Torresan, M.E., 1999, Stratigraphic constraints on the timing and emplacement of the Alike 2 giant Hawaiian submarine landslide: *Journal of Volcanology and Geothermal Research*, v. 94, p. 35-58.
- Moore, J.G. and Clague, D.A., 2002, Mapping the Nuanu and Wailau landslides in Hawaii, *in* Takahashi, E., Lipman, P.W., Garcia, M.O., Naka, J. and Aramaki, S., eds., *Hawaiian Volcanoes, Deep Water Perspectives*: Geophysical Monograph 128, American Geophysical Union, Washington DC, p. 223-244.
- Moore, J.G., Normark, W.R. and Holcomb, R.T., 1994, Giant Hawaiian landslides: *Annual Review of Earth and Planetary Sciences*, v. 22, p. 119-144.
- Morgan, W.J., 1971, Convection plumes in the lower mantle, *Nature*, v. 230, p. 42-43.
- Mullineaux, D.R., Peterson, D.W. and Crandell, D.R., 1987, Volcanic hazards in the Hawaiian Islands, *in* Decker, R.W., Wright, T.L. and Stauffer, P.H., eds., *Volcanism in Hawaii*, U.S. Geological Survey Professional Paper 1350, v. 1, p. 599-621.
- Nisbet, E.G. and Pearce, J.A., 1977, Clinopyroxene composition in mafic lavas from different tectonic settings: *Contributions to Mineralogy and Petrology*, v. 63, p. 149-160.
- Philpotts, A.R., 1990, *Principles of Igneous and Metamorphic Petrology*: Prentice Hall, Englewood Cliffs, New Jersey, 498 p.
- Pietruszka, A.J. and Garcia, M.O., 1999, The size and shape of Kilauea Volcano's summit magma storage reservoir: a geochemical probe: *Earth and Planetary Science Letters*, v. 167, p. 311-320.
- Prestvik, T., Goldberg, S., Karlsson, H., Gronvold, K., 2001, Anomalous strontium and lead isotope signatures in the off-rift Oraefajokull central volcano in South-east Iceland; evidence for enriched endmember(s) of the Iceland mantle plume? *Earth and Planetary Science Letters*, v. 190, p. 211-220.
- Reid, M.R., 2003, Timescales of Magma transfer and storage in the crust, *in* Rudnick, R.L. ed., *The Crust*: Holland, H.D. and Turekian, K.K., eds., Volume 3, *Treatise on Geochemistry*: Elsevier-Pergamon, Oxford, p. 167-193.
- Renzulli, A. and Santi, P., 2000, Two-stage fractionation history of the alkali basalt-trachyte series of Sete Cidades volcano (São Miguel Island, Azores): *European Journal of Mineralogy*, v. 12, p. 469-494.
- Sen, G., Macfarlane, A. and Srimal, N., 1996, Significance of rare hydrous alkaline melts in Hawaiian xenoliths: *Contributions to Mineralogy and Petrology*, v. 122, p. 415-427.
- Sigmarrsson, O., 1996, Short magma chamber residence time at an Icelandic volcano

- inferred from U-series disequilibria:  
*Nature*, v. 382, p. 440-442.
- Tatsumi, Y., Oguri, K., Shimoda, G., Kogiso, T. and Barszczus, H.G., 2000, Contrasting behavior of noble-metal elements during magmatic differentiation in basalts from the Cook Islands, *Polynesia: Geology*, v. 28, p. 131-134.
- Thompson, G.M., Smith, I.E.M. and Malpas, J.G., 2001, Origin of oceanic phonolites by crystal fractionation and the problem of the Daly gap: an example from Rarotonga: *Contributions to Mineralogy and Petrology*, v. 142, p. 336-346.
- Watson, S. and McKenzie, D., 1991, Melt generation by plumes; a study of Hawaiian volcanism: *Journal of Petrology*, v. 32, p. 501-537.
- West, H.B., Garcia, M.O., Frey, F.A. and Kennedy, A., 1988, Nature and cause of compositional variation among the alkalic cap lavas of Mauna Kea Volcano, Hawaii: *Contributions to Mineralogy and Petrology*, v. 100, p. 383-397.
- Williams, H. and McBirney, A.R., 1987, *Volcanology*, Freeman, Cooper & Co., San Francisco, 397 p.
- Wilson, J.T., 1963, A possible origin of the Hawaiian Islands: *Canadian Journal of Physics*, v. 41, p. 863-870.
- Wilson, J.T., 1973, Mantle plumes and plate motions: *Tectonophysics*, v. 19, p. 149-164.
- Wolff, J.A., Grandy, J.S. and Larson, P.B., 2000, Interaction of mantle-derived magma with island crust? Trace element and oxygen isotope data from the Diego Hernandez Formation, Las Canadas, Tenerife: *Journal of Volcanology and Geothermal Research*, v. 103, p. 343-366.
- Zhao, D., 2001, Seismic structure and origin of hotspots and mantle plumes: *Earth and Planetary Science Letters*, v. 192, p. 251-265.

Accepted as revised 1 Dec 2004